NO RECORD

NACA RM No. L8F30

AAB 3302

AERONAUTICS LIBRARY
California Institute of Technology

NACA

RESEARCH MEMORANDUM

APPLICATION OF THEODORSEN'S THEORY TO PROPELLER DESIGN

By

John L. Crigler

Langley Aeronautical Laboratory
Langley Field, Va.

NATIONAL ADVISORY COMMITTEE
FOR AERONAUTICS

WASHINGTON
July 26, 1948

NACA RM No. L8F30

NATIONAL ADVISORY COMMITTEE FOR AERONAUTICS

RESEARCH MEMORANDUM

APPLICATION OF THEODORSEN'S THEORY TO PROPELLER DESIGN

By John L. Crigler

SUMMARY

A theoretical analysis is presented for obtaining by use of Theodorsen's propeller theory the load distribution along a propeller radius to give the optimum propeller efficiency for any design condition. The efficiencies realized by designing for the optimum load distribution are given in graphs, and the optimum efficiency for any design condition may be read directly from the graph without any laborious calculations. Examples are included to illustrate the method of obtaining the optimum load distributions for both single-rotating and dual-rotating propellers.

INTRODUCTION

Recent contributions to the theory of propellers have been made by Theodorsen in a series of reports (references 1 to 4). In the first report of the series (reference 1) a method based on electrical analogy was devised for obtaining the ideal circulation functions for single-rotating propellers. These circulation functions were shown to be in good agreement with the theoretical calculations made by Goldstein in reference 5 for two- and four-blade single-rotating propellers and with the extrapolations to other numbers of blades made by Lock and Yeatman in reference 6. The electrical-analogy method of measuring these functions was also applied to more difficult cases for which no theoretical calculations had previously been made; in particular, to the case of dual-rotating propellers.

Theodorsen in reference 1 introduced the concept of the mass coefficient κ, which is an integrated value of the circulation functions. The mass coefficient represents the effective cross section of the column of the medium pushed by the propeller divided by the projected-propeller-wake area.

This mass coefficient is made use of in the development of Theodorsen's theory. In reference 4, expressions are given for computing the thrust, the energy loss, and the efficiency of any propeller with ideal circulation distribution based on the conditions in the final wake in terms of the mass coefficient. It is of interest to mention that the mass coefficient or mass of air operated on by the dual-rotating propeller

is much greater than that affected by the single-rotating propeller for the same set of operating conditions. This large difference in the mass coefficients for the two cases indicates that calculations for dual-rotating propellers based on the ideal circulation functions for single-rotating propellers are inadequate.

Theodorsen's theory, as previously mentioned, is based on the conditions in the final wake. The present analysis attempts to interrelate the conditions in the final wake to the propeller and to give the information necessary to design a propeller for any desired operating condition. For single-rotating propellers, the method yields the same results as the conventional vortex theory with the Goldstein tip corrections applied. By the conventional vortex theory, however, it is necessary to determine the optimum blade-load distribution and then to make element strip-theory calculations in order to obtain the optimum efficiency for a given design condition. This procedure has been followed in reference 7 for a wide range of operating conditions. By Theodorsen's theory the optimum efficiency η can be obtained directly for any design condition from its relationship to the mass coefficient without laborious calculations. Thus, in the selection of a propeller for any design condition, a close estimate of the efficiency can be obtained before the design is made.

The circulation functions and mass coefficients for the dual-rotating propeller were obtained in reference 1 for the ideal case and refer to conditions in the ultimate wake. Both propellers were assumed to operate in the same plane. Obviously, this condition is unattainable in the design of an actual propeller. The degree to which the ideal case can be realized in practice, or the applicability of the ideal functions to a given case, require further consideration and confirmation.

SYMBOLS

B	number of propeller blades
b	chord of propeller-blade element
c_d	section drag coefficient
c_l	section lift coefficient
P_c	ideal power coefficient $(c_s + e)$
P_{c_T}	total-power coefficient $(P_c + t_r)$
c_s	thrust coefficient $\left(\frac{T}{\frac{1}{2}\rho V^2 F}\right)$

c_{s_T}	net thrust coefficient $(c_s - t_a)$
D	diameter of propeller
d	drag of propeller section
D_o	diameter of wake helix surface
E	ideal energy loss in wake $\left(\rho F \kappa w^2 \left(\frac{\epsilon}{\kappa} w + \frac{1}{2} V\right)\right)$
E_D	energy loss due to blade drag
e	induced energy loss coefficient $\left(\frac{E}{\frac{1}{2}\rho V^3 F}\right)$
F	projected area of helix (at infinity)
K(x)	circulation function
l	lift of propeller section
n	propeller rotational speed, revolutions per second
P	input power to propeller
R	tip radius
r	radius to any blade element
T	thrust of propeller
t	power loss due to drag (nondimensional)
t_a	axial power loss due to drag
t_r	rotational power loss due to drag
V	forward axial velocity of propeller
V_a	axial interference velocity (at propeller)
$\bar{V}_a$	average axial interference velocity (at propeller)
V_i	resultant interference velocity (at propeller)
V_r	rotational interference velocity (at propeller)

$\bar{V}_r$ average rotational interference velocity (behind each propeller)

W resultant velocity on the propeller at radius r

W_S local self-interference velocity

w rearward displacement velocity of helical vortex surface

$\bar{w}$ ratio of displacement velocity to forward velocity (w/V)

x radial location of blade element (r/R)

α angle of attack, degrees

α_i induced angle of attack, degrees

β blade angle, degrees

λ advance ratio $\left(\frac{1}{\pi}\frac{V + w}{nD_o}\right)$

λ_g geometric advance ratio $(V/\pi nD)$

κ mass coefficient $\left(2\int_0^1 K(x)x\,dx\right)$

ϵ axial energy loss factor

η propeller efficiency $\left(\frac{c_s - t_a}{P_c + t_r}\right)$

η_i ideal propeller efficiency $\left(c_s/P_c\right)$

ρ mass density of air

σ propeller element solidity $(Bb/2\pi r)$

σc_l propeller element load coefficient

Γ circulation at radius x $\left(\Gamma(x) = \frac{2\pi(V + w)w}{B\omega}K(x)\right)$

φ angle of resultant velocity W at plane of rotation

$\varphi_o = \tan^{-1}\frac{V/nD}{\pi x}$

ω angular velocity

Subscripts:

F	front
R	rear
0.7R	at 0.7 radius

OPTIMUM PROPELLER DESIGN

Single-Rotating Propellers

Velocity diagram.- The velocity diagram for the single-rotating propeller is shown in figure 1. This figure is a reproduction of figure 13, reference 2, with some additional designations. The relationship between the axial interference velocity at the radius r, as given by the vortex theory, to the displacement velocity w of the vortex sheet is calculated in reference 2 and is shown in figure 1. The forward axial velocity of the propeller is V and the tangential velocity with respect to the air at rest is ωr. The vector $\overline{bd}$ is the resultant interference velocity V_i of the air with respect to the air at rest. Thus, the resultant velocity W of a point on the propeller at the radius r is given by the vector $\overline{cd}$. The lift force l is perpendicular to this vector and the drag force d is exactly opposite in direction to W as indicated. From this figure a comparison of the method of analysis presented herein may be made with the conventional vortex-theory method. It is required to find the point d in order to locate the end of the velocity vector W and the angle φ that the vector W makes with the direction of rotation. By the conventional vortex theory, the point d is located by starting with point b obtained from the V/nD of the undisturbed flow, proceeding in the V direction the distance V_a, and then taking the perpendicular to this direction a distance V_r. (See reference 8.) The angle φ is given by $\tan \varphi = \dfrac{V + V_a}{\omega r - V_r}$ and $W = \dfrac{V + V_a}{\sin \varphi}$. In the calculation of interference velocities V_a and V_r the local tip correction or Goldstein factor must be used to obtain the correct location of the point d.

With the method developed in references 1 to 4, only the value of $\frac{1}{2} w$, which remains constant with radius, need be used. With this concept it is possible to use the integrated values of the mass coefficient as determined by the electrical analogy of reference 1 to obtain the detailed information needed at any radius. By this method the point d can be located by proceeding from point b a distance $\frac{1}{2} w$ in the V direction to the point e and then down the direction of the

velocity vector W a distance $\overline{de}$, where $\overline{de}$ is obtained from the geometry of the figure as $\frac{1}{2} w \sin \varphi$ and

$$\tan \varphi = \frac{V + \frac{1}{2} w}{\omega r} \tag{1}$$

The resultant velocity is

$$W = \frac{V + \frac{1}{2} w}{\sin \varphi} - \frac{1}{2} w \sin \varphi$$

$$= \frac{1}{\sin \varphi} \left(V + \frac{1}{2} w \cos^2 \varphi \right) \tag{2}$$

The interference velocities may be obtained from the geometry of the figure by

$$V_i = \frac{1}{2} w \cos \varphi$$

$$V_a = V_i \cos \varphi = \frac{1}{2} w \cos^2 \varphi$$

and

$$V_r = V_i \sin \varphi = \frac{1}{2} w \sin \varphi \cos \varphi$$

Optimum blade-load distribution.- The design problem of an optimum propeller consists essentially in obtaining the value of the element load coefficient bc_l at each radius of the propeller blade. With the direction and magnitude of the relative velocity given at each station there remains only the choice of a section to give efficiently such a lift at the appropriate angle of attack. The value of c_l should be at or near the ideal lift coefficient for the section in order to give minimum drag coefficient.

The method developed in references 1 to 4 treats the velocity w as an independent parameter upon which all the other quantities depend. This reversal of procedure is convenient since all quantities are actually functions of w. The velocity w is related to the power coefficient P_c of the propeller and also to the element load coefficient σc_l. The relation of w to σc_l is developed herein and the

relation of w to P_c, which must be obtained in order to use it for design, is given subsequently in the section "PROCEDURE FOR PROPELLER DESIGN."

The required ideal circulation $\Gamma(x)$ is given in reference 1 by

$$\Gamma(x) = \frac{2\pi(V + w)w}{B\omega} K(x)$$

$$= \frac{(V + w)w}{Bn} K(x) \tag{3}$$

In order to determine the element load coefficient bc_l the relation for the equality of the force on a vortex element and on an element of a lifting surface is given as

$$\rho\Gamma W = \frac{1}{2} \rho W^2 c_l b$$

where b is the chord of the element. Hence,

$$\Gamma = \frac{1}{2} W c_l b \tag{4}$$

where W is given in equation (2), and thus

$$\Gamma = \frac{1}{2} \frac{1}{\sin \varphi} \left(V + \frac{1}{2} w \cos^2 \varphi \right) c_l b \tag{5}$$

Using equations (3) and (5) for Γ gives at once the identity

$$bc_l = \frac{(V + w)w}{Bn} K(x) \frac{2 \sin \varphi}{V + \frac{1}{2} w \cos^2 \varphi}$$

Introducing the nondimensional velocity $\bar{w} = \frac{w}{V}$, the solidity $\sigma = \frac{Bb}{2\pi r}$, and $\tan \varphi = \frac{V + \frac{1}{2} w}{2\pi rn}$ (equation (1)) gives the nondimensional relation

$$\sigma c_l = \frac{1 + w}{\left(1 + \frac{1}{2}\bar{w}\right)\left(1 + \frac{1}{2} w \cos^2\varphi\right)} 2\bar{w}K(x) \frac{\sin^2\varphi}{\cos\varphi} \qquad (6)$$

The selection of a propeller for a given airplane installation may be based on a method of evaluating a series of propellers for various operating conditions in order to determine the most suitable propeller. It is probable that several propellers, varying in diameter, blade number, propeller operational speed, and direction of rotation are equally as efficient for the design condition so that other considerations may enter into the propeller selection. However, the optimum efficiency for the propeller selected may be obtained from the charts, and therefore the load distribution along the radius that will give this optimum efficiency remains to be determined.

The value of σc_l may be calculated for any radius from the relation

$$\sigma c_l = \frac{1 + \bar{w}}{\left(1 + \frac{1}{2}\bar{w}\right)\left(1 + \frac{1}{2}\bar{w} \cos^2\varphi\right)} 2\bar{w}K(x) \frac{\sin^2\varphi}{\cos\varphi}$$

where

$$\varphi = \tan^{-1} \frac{1}{\pi} \frac{V}{nD} \frac{1 + \frac{1}{2}\bar{w}}{x} = \tan^{-1} \lambda_g \frac{1 + \frac{1}{2}\bar{w}}{x} \qquad (7)$$

Dual-Rotating Propellers

In the design of dual-rotating propellers, it has been customary to select two propellers designed for single rotation and to use them as a dual-rotating propeller. The fact that the circulation functions and the mass coefficients obtained by the electrical-analogy method (reference 1) are very much larger for the dual-rotating propeller than the sum of the values for the two single-rotating propellers indicates that the functions as used heretofore are not proper. The electrical-analogy method represents the case of an idealized dual-rotating propeller in which the two components are in the same plane with the same load distribution on each component and with equal power absorption. Since actual propellers cannot conform to this ideal case, the applicability of the ideal functions requires further confirmation. Nevertheless, the optimum distribution for the dual-rotating propeller is essentially different from the single-rotating propeller, and in this analysis the loading functions and the mass coefficients as determined by the electrical-analogy method are assumed to apply to the optimum dual-rotating propeller.

Interference velocities for dual-rotating propellers.- The average axial interference velocity far behind the propeller obtained from the momentum considerations is

$$2\bar{V}_a = \kappa w$$

where κ is the mass coefficient and w is the axial displacement velocity. This mean value is equally due to each of the two oppositely rotating propellers. The average axial interference velocity due to each is therefore exactly

$$\bar{V}_a = \frac{1}{2} \kappa w$$

The average interference velocity at the propeller plane is one-half the value in the final wake and, therefore,

$$\frac{1}{2} \bar{V}_a = \frac{1}{4} \kappa w$$

where $\frac{1}{2} \bar{V}_a$ represents the average axial interference velocity at the propeller plane due to each component of the dual-rotating propeller. With the two propellers separated by a small axial distance, this velocity refers to a plane between the two propellers. The interference velocity at the front propeller is smaller and at the rear propeller is larger than at the plane between the propellers. In the following treatment, the propellers are considered to be very close together so that the axial interference velocity is the same on both propellers.

In the final wake, the mean value of the rotational interference velocity for the ideal case is given by

$$2\bar{V}_r = 0$$

For an infinite number of right and left blades equally loaded, rotational components would cancel exactly. However, the average rotational interference velocity immediately behind each propeller may be considered as

$$\bar{V}_r = \frac{1}{2} \kappa w \tan \varphi$$

In summary, the mean interference velocities acting on the front propeller from the rear propeller are:

Axial: $\frac{1}{2}\bar{V}_a = \frac{1}{4}\kappa w$

Rotational: $\bar{V}_r = 0$

The mean interference velocities acting on the rear propeller from the front propeller are:

Axial: $\frac{1}{2}\bar{V}_a = \frac{1}{4}\kappa w$

Rotational: $\bar{V}_r = \frac{1}{2}\kappa w \tan \varphi$

It is useful to recognize that the mean self-interference of each propeller in its own plane is

Axial: $\frac{1}{4}\kappa w$

Rotational: $\frac{1}{4}\kappa w \tan \varphi$

Velocity diagram for the dual-rotating propellers.- The velocity diagram for the dual-rotating propellers is shown in figure 2. As in the case for the single-rotating propeller, the axial displacement velocity at the propeller is equal to $\frac{1}{2}w$. In figure 2 the vector $\overline{AB}$ gives the mean axial interference velocity $\frac{1}{4}\kappa w$ of each propeller acting on the other propeller. The vector $\overline{BC}$ gives the mean rotational interference velocity $\frac{1}{2}\kappa w \tan \varphi$ of the front propeller acting on the rear propeller. The total interference velocity acting on the front propeller from the rear propeller is therefore given by $\overline{AB}$, and the total interference velocity acting on the rear propeller from the front propeller is equal to the vector $\overline{AC}$. The local self-interference velocity of the front propeller is given by W_{S_F}, and the corresponding helix angle is given by φ_F. The local self-interference velocity of the

rear propeller is given by W_{S_R}, and the corresponding helix angle is given by φ_R. The angle φ_F is slightly larger than the ideal helix angle φ given by the displacement velocity $\frac{1}{2}w$ and φ_R is slightly smaller than φ. The design condition of most interest is the one for which Γ_F for each blade of the front propeller is equal to Γ_R for each blade of the rear propeller. The number of blades on the front and rear propeller are considered equal and the rotational speeds the same. This condition gives the self-interference velocity on the front propeller equal to the self-interference velocity on the rear propeller and means that D and E must be at the same horizontal level.

As φ_F and φ_R are needed in the design of the propeller, it is seen from figure 2 that the associated displacement velocity on the front and rear propellers has been increased and decreased, respectively, by the amount

$$\Delta w = \frac{1}{4}\kappa w \tan^2\varphi$$

The displacement velocity is therefore

Front: $$\frac{1}{2}w\left(1 + \frac{1}{2}\kappa \tan^2\varphi\right)$$

Rear: $$\frac{1}{2}w\left(1 - \frac{1}{2}\kappa \tan^2\varphi\right)$$

From figure 2, the velocity W_F is shown to be given by the relationship

$$W_F = \frac{V}{\sin \varphi_o} + \frac{1}{4}\kappa w \sin \varphi_o$$

$$= \frac{V}{\sin \varphi_o}\left(1 + \frac{1}{4}\kappa \bar{w} \sin^2\varphi_o\right) \qquad (8)$$

and the angle φ_F is given by

$$\tan \varphi_F = \frac{V + \frac{1}{2} w\left(1 + \frac{1}{2} \kappa \tan^2\varphi\right)}{\omega r}$$

$$= \frac{V}{nD} \frac{1}{\pi x}\left[1 + \frac{1}{2} \bar{w}\left(1 + \frac{1}{2} \kappa \tan^2\varphi\right)\right] \tag{9}$$

where φ is given by the relationship

$$\tan \varphi = \frac{V + \frac{1}{2} w}{\omega r}$$

$$= \frac{V}{nD} \frac{1}{\pi x}\left(1 + \frac{1}{2} \bar{w}\right)$$

Similarly,

$$W_R = \frac{V}{\sin \varphi_o} + \frac{1}{4} \kappa w \sin \varphi_o + \frac{1}{2} \kappa w \tan \varphi_o \cos \varphi_o$$

$$= \frac{V}{\sin \varphi_o} + \frac{3}{4} \kappa w \sin \varphi_o$$

$$= \frac{V}{\sin \varphi_o}\left(1 + \frac{3}{4} \kappa \bar{w} \sin^2\varphi_o\right) \tag{10}$$

and

$$\tan \varphi_R = \frac{V + \frac{1}{2} w\left(1 - \frac{1}{2} \kappa \tan^2\varphi\right)}{\omega r}$$

$$= \frac{V}{nD} \frac{1}{\pi x}\left[1 + \frac{1}{2} \bar{w}\left(1 - \frac{1}{2} \kappa \tan^2\varphi\right)\right] \tag{11}$$

Optimum blade-load distribution.- The optimum distribution of blade loading is obtained from the determination of the element load coefficient bc_l at each radius from the fundamental relation

$$\frac{1}{2} \rho b c_l W^2 = \rho \Gamma W$$

where Γ has been given in equation (3) by

$$\Gamma = \frac{(V + w)w}{Bn} K(x)$$

Eliminating Γ gives

$$\frac{1}{2} Bbc_l W = \frac{(V + w)w}{n} K(x)$$

but $\frac{1}{2}\frac{Bb}{2\pi r} = \sigma$ is the solidity of each component of the dual-rotating propeller, if the number of blades in each component are assumed to be equal. Therefore,

$$\sigma c_l W = \frac{V}{\pi n D x}(1 + \bar{w})\bar{w}V \, K(x)$$

For the front propeller, this equation may be solved by use of equation (8) and

$$\left(\sigma c_l\right)_F = \frac{V}{nD}\frac{1}{\pi x}\frac{(1 + \bar{w})\bar{w} \sin \varphi_o}{1 + \frac{1}{4}\kappa\bar{w} \sin^2\varphi_o} K(x) \tag{12}$$

and for the rear propeller by use of equation (10)

$$\left(\sigma c_l\right)_R = \frac{V}{nD}\frac{1}{\pi x}\frac{(1 + \bar{w})\bar{w} \sin \varphi_o}{1 + \frac{3}{4}\kappa\bar{w} \sin^2\varphi_o} K(x) \tag{13}$$

Use of Design Formulas

In order to use the relation for σc_l, note that it contains not only the independent variable $\bar{w}$ but also the function $K(x)$ and the angle φ. The parameter $K(x)$ should be expressed as a function of $\frac{V + w}{nD_o}$, which is based on the wake helix diameter. As was shown in reference 3, however, D_o differs only slightly from the propeller diameter D and in the present design procedure D is used instead of D_o. The function $K(x)$

for single-rotating propellers is plotted against $\frac{V + w}{nD}$ in figures 3 to 7. Similar plots for dual-rotating propellers were taken from reference 1 and are presented in figures 8 to 10.

EQUATIONS FOR PERFORMANCE CALCULATIONS

Single-Rotating Propellers

In reference 4 the thrust has been given by

$$T = \rho F \kappa w \left[V + w \left(\frac{1}{2} + \frac{\epsilon}{\kappa} \right) \right]$$

and the ideal energy loss in the wake has been given by

$$E = \rho F \kappa w^2 \left(\frac{\epsilon}{\kappa} w + \frac{1}{2} V \right)$$

With the introduction of the nondimensional quantity $\bar{w} = \frac{w}{V}$, the thrust coefficient in nondimensional form is

$$c_s = \frac{T}{\frac{1}{2} \rho V^2 F}$$

$$= 2\kappa\bar{w} \left[1 + \bar{w} \left(\frac{1}{2} + \frac{\epsilon}{\kappa} \right) \right] \tag{14}$$

and the induced loss coefficient is

$$e = \frac{E}{\frac{1}{2} \rho V^3 F}$$

$$= 2\kappa\bar{w}^2 \left(\frac{1}{2} + \frac{\epsilon}{\kappa} \bar{w} \right) \tag{15}$$

The power coefficient $P_c = c_s + e$ is given by

$$P_c = 2\kappa\bar{w}(1 + \bar{w})\left(1 + \frac{\epsilon}{\kappa}\bar{w}\right) \tag{16}$$

The efficiency is given by

$$\eta_i = \frac{c_s}{P_c} \tag{17}$$

These formulas are all that are necessary for single-rotating propellers. The performance of the dual-rotating propeller is computed by the same formulas.

Dual-Rotating Propellers

The thrust of the front propeller is given by

$$dT_F = \frac{1}{2}\rho(2\pi r)W_F^2\left(\sigma c_l\right)_F \cos\varphi_F \, dr$$

and with $\left(\sigma c_l\right)_F$ from equation (12) and W_F from equation (8)

$$T_F = \rho\frac{D}{4}V^3\bar{w}(1 + \bar{w})\frac{1}{n}\int_0^1\left(1 + \frac{1}{4}\kappa\bar{w}\sin^2\varphi_o\right)\frac{\cos\varphi_F}{\sin\varphi_o}K(x)\,dx \tag{18}$$

Similarly, for the rear propeller

$$T_R = \rho\frac{D}{4}V^3\bar{w}(1 + \bar{w})\frac{1}{n}\int_0^1\left(1 + \frac{3}{4}\kappa\bar{w}\sin^2\varphi_o\right)\frac{\cos\varphi_R}{\sin\varphi_o}K(x)\,dx \tag{19}$$

The coefficients c_s, e, and P_c for the dual-rotating propellers are given in the same form as in equations (14), (15), and (16) for single-rotating propellers. The only difference in the coefficients results from differences in the values of κ, $\bar{w}$, and ϵ/κ which are substituted in the equations.

Blade-Drag Losses

The frictional loss or loss in efficiency due to the profile drag of the blade is

$$E_D = B \frac{\rho}{2} \int_0^R bc_d W^3 \, dr$$

The drag force per unit length is $\frac{1}{2} \rho W^2 bc_d$ where W, the resultant velocity of the blade element, has been given in equation (2) for single-rotating propellers by

$$W = \frac{1}{\sin \varphi} \left(V + \frac{1}{2} w \cos^2 \varphi \right)$$

For the design condition, w is small, and because of the obvious uncertainties in the determination of the value of c_d, it is not necessary to retain the second term $\frac{1}{2} w \cos^2 \varphi$. Introducing the solidity factor $\sigma = \frac{Bb}{2\pi r}$ permits the drag loss to be given by

$$E_D = \pi R^2 \rho V^3 \int_0^1 \frac{\sigma c_d}{\sin^3 \varphi} x \, dx$$

or in nondimensional form

$$t = \frac{E_D}{\frac{1}{2} \rho V^3 \pi R^2}$$

$$= 2 \int_0^1 \frac{\sigma c_d}{\sin^3 \varphi} x \, dx \qquad (20)$$

The component power losses are then, to the same degree of approximation in nondimensional form,

Rotational: $$t_r = \frac{2}{\lambda_g^2} \int_0^1 \frac{\sigma c_d}{\sin \varphi} x^3 \, dx \tag{21}$$

Axial: $$t_a = 2 \int_0^1 \frac{\sigma c_d}{\sin \varphi} x \, dx \tag{22}$$

For the dual-rotating propeller operating at the design conditions, the terms containing w are small, as is the case with the single-rotating propeller, and a close approximation to the drag loss is obtained if these terms are neglected. Furthermore, if it is assumed that the average of the resultant velocity W for the dual combination is equal to W for the single propeller, the equations (20) to (22) may be used for the dual-rotating propellers. Of course, for conditions other than the design condition, especially for very heavy loadings, exact drag-loss claculations require that the exact equations be used for either single-rotating or dual-rotating propellers.

In summary, the equations for obtaining the propeller performance are given by the quantities c_s, e, and P_c and the drag-loss factors are given by t_r and t_a.

The net thrust power is

$$c_{s_T} = c_s - t_a \tag{23}$$

The power input is

$$P_{c_T} = c_s + e + t_r = P_c + t_r \tag{24}$$

The efficiency is

$$\eta = \frac{c_s - t_a}{P_c + t_r} = \frac{c_{s_T}}{P_{c_T}} \tag{25}$$

where from equation (16)

$$P_c = 2\kappa\bar{w}(1 + \bar{w})\left(1 + \frac{\epsilon}{\kappa}\bar{w}\right)$$

The total power is also given by

$$P = \frac{1}{2}\rho V^3 \pi R^2 P_{c_T} \tag{26}$$

It should be remembered that the calculation is based on a given $\bar{w}$. This procedure may seem unjustifiable since this parameter is not given by the specification but is the end result of a calculation based on the original data. The induced loss does not depend on the total-power coefficient P_{c_T}, but actually depends only on P_c, and the quantity $\bar{w}$ cannot be obtained from the total-power coefficient. However, the value of P_{c_T} in most cases exceeds P_c by not more than 2 percent or

$$P_c = 0.98\, P_{c_T}$$

Since P_c in equation (16) is based on the $\bar{w}$ and the diameter of the final wake, and the value of P_{c_T} in equation (24) is based on the propeller diameter which is slightly larger than the diameter of the final wake, a very close approximation to $\bar{w}$ is usually given by equation (16). Therefore,

$$P_{c_T} \approx P_c = 2\kappa\bar{w}(1 + \bar{w})\left(1 + \frac{\epsilon}{\kappa}\bar{w}\right)$$

In some cases it may be necessary to calculate t_r to obtain a more exact value of P_c, especially if the blade profile drag is large.

PROCEDURE FOR DESIGN OF PROPELLER

Figures Used in Propeller Design

The information necessary to design a propeller for any operating condition is given in the figures. Figures 3 to 7 give the circulation function $K(x)$ interpolated for even fractions for two-, three-, four-, six-, and eight-blade single-rotating propellers. The circulation function for the two-blade propeller was taken directly from reference 5; for the three-blade propeller, from reference 6; and for the propellers having a greater number of blades was recalculated from the Goldstein tip correction factors as given in reference 7. Figures 8, 9, and 10 give $K(x)$ for dual-rotating propellers with four, eight, and twelve blades, respectively. These values for the dual-rotating propellers

were taken from reference 1. Figure 11 gives the mass coefficient κ for various numbers of blades for single-rotating propellers. Figure 12, which was taken from reference 1, gives κ for dual-rotating propellers. The ideal efficiency η_i is plotted against $\bar{w}$ for a range of values ϵ/κ in figure 13, against c_s/κ in figure 14, and against P_c/κ in figure 15. The data for figures 13 and 14 were taken directly from reference 4 and the data for figure 15 was recalculated by the use of equation (16) and figure 13. Figures 13 to 15 apply to either single- or dual-rotating propellers. The propeller efficiency may be calculated from either of these figures; however, in this report the efficiency has been determined from P_c/κ as given in figure 15.

Figures 16 and 17 give values of ϵ, κ, and ϵ/κ for two- and four-blade single-rotating propellers and figures 18 to 20 give values for four-, eight-, and twelve-blade dual-rotating propellers. The values of ϵ for a propeller with a finite number of blades have not previously been published, but the values of ϵ and ϵ/κ for an infinite number of blades are given in figure 4 of reference 4. The method for calculating ϵ/κ and ϵ is given in the following section.

Propeller Selection

In the selection of a propeller for a given airplane installation, the engine power, the forward speed, and the design altitude are usually specified. The selection consists of the determination of the number of blades, the propeller solidity, the propeller diameter, and the rotative speed. The ideal propeller efficiency for any combinations of these variables can be readily obtained with the use of the charts. The procedure for a given blade number, propeller diameter, and rotative speed for either single or dual rotation is as follows:

First, calculate the total-power coefficient

$$P_{c_T} = \frac{P}{\frac{1}{2}\rho V^3 \frac{\pi}{4} D^2}$$

and then use this value for the ideal coefficient

$$P_{c_T} \approx P_c = 2\kappa\bar{w}(1 + \bar{w})\left(1 + \frac{\epsilon}{\kappa}\bar{w}\right)$$

to find $\bar{w}$.

It was shown in reference 4 that the dependence of the efficiency on ϵ/κ in the efficiency formulas is very small and that it is sufficient to know only the approximate value of ϵ/κ. An examination of the formulas for c_s and P_c shows that their dependence on ϵ/κ is also small. It was further concluded in reference 4 that ϵ/κ is only slightly greater than κ and that the practice of using ϵ/κ instead of κ is considered satisfactory for design purposes. However, there appears to exist a simple relation between the axial-loss factor ϵ and the total-loss factor κ. This relation takes on the form of a differential equation

$$\frac{\epsilon}{\kappa} = 1 + \frac{1}{2}\frac{\lambda}{\kappa}\frac{d\kappa}{d\lambda}$$

where

$$\lambda = \frac{1}{\pi}\frac{V + w}{nD_o}$$

This relation has been checked and found to be exact for an infinite number of blades, and numerical checks for a two-blade propeller were in very close agreement. It is considered accurate for an empirical relation for design purposes for propellers of other numbers of blades.

First obtain

$$\lambda_g = \frac{1}{\pi}\frac{V}{nD}$$

as a first approximation to λ for use in the calculations. Then read off κ and $d\kappa/d\lambda$ from the appropriate charts of κ against $\frac{V}{nD}(1 + \bar{w})$ for several values of $\bar{w}$ (figs. 11 and 12). Curves of ϵ, κ, and ϵ/κ are plotted against $\frac{V}{nD}(1 + \bar{w})$ in figures 16 to 20. Next plot a curve for the right side of the equation for P_c against $\bar{w}$. Where this curve intersects the horizontal line, $P_c = P_{c_T}$ is the desired point. This value may be checked from the chart by inserting the values obtained from the plot in the equation. Thus are obtained κ, $\bar{w}$, $\frac{V}{nD}(1 + \bar{w})$, and ϵ/κ. From the chart of P_c/κ (fig. 15), the optimum efficiency may be obtained.

The following examples illustrate the method of determining the optimum distribution of bc_l along the radius for both single-rotating and dual-rotating propellers that give the maximum possible efficiency (neglecting blade profile drag) that can be obtained with either propeller for one specified design condition.

Illustrative Examples

Single rotation.- Let the following data specify the propeller design conditions:

Power, horsepower	2000
Density, slugs per cubic foot	0.001065
Velocity, miles per hour	425

The propeller selection has been made to the extent that the following data specify the propeller:

Rotational speed, n, revolutions per second	23
Propeller diameter, D, feet	12
Number of blades, B	4
V/nD	2.258

The total P_{c_T} from the given conditions is

$$P_{c_T} = \frac{P}{\frac{1}{2}\rho V^3 \pi R^2}$$

$$= \frac{(2000)(550)}{\frac{1}{2}(0.001065)(623)^3\pi(6)^2} = 0.075$$

The value of P_c should be based on the wake diameter D_o instead of on the propeller diameter D and used to calculate $\bar{w}$. Both P_c and the contraction may be obtained by successive approximations but the two effects tend to cancel each other and generally P_{c_T} based on the propeller diameter is sufficiently accurate to use in the calculation of $\bar{w}$. The relation between $\bar{w}$ and P_c is given by equation (16) as

$$P_c = 2\kappa\bar{w}(1 + \bar{w})\left(1 + \frac{\epsilon}{\kappa}\bar{w}\right)$$

where

$$P_c = P_{c_T}$$

If values of $\bar{w}$ are selected to cover the range and the curve for the four-blade propeller in figure 17 is used, the following table is obtained for the four-blade single-rotating propeller:

$\bar{w}$ (assumed)	κ	ϵ/κ	P_c
0	0.245	0.340	0
.1	.215	.313	.0488
.2	.191	.289	.0970

A plot of P_c against $\bar{w}$ gives a value of $\bar{w} = 0.155$ at $P_c = 0.075$. Then,

$$\frac{V}{nD}(1 + \bar{w}) = (2.258)(1.155) = 2.61$$

From figure 17, κ is read at $\frac{V}{nD}(1 + \bar{w}) = 2.61$, and the optimum propeller efficiency η_i for a four-blade single-rotating propeller is read from figure 15. Thus

$$\kappa = 0.201$$

$$\frac{P_c}{\kappa} = 0.373$$

and

$$\eta_i = 0.929$$

With $\bar{w}$ determined, σc_l for the single-rotating propeller may be found by a direct calculation from equation (6)

$$\sigma c_l = \frac{1 + \bar{w}}{\left(1 + \frac{1}{2}\bar{w}\right)\left(1 + \frac{1}{2}\bar{w}\cos^2\varphi\right)} 2\bar{w}\, K(x) \frac{\sin^2\varphi}{\cos\varphi}$$

Values of the circulation function $K(x)$ at each station are obtained from figure 4 at $\frac{V}{nD}(1 + \bar{w}) = 2.61$ and the angle of the relative velocity at the propeller is given for each station by

$$\tan\varphi = \frac{1}{\pi}\frac{V}{nD}\frac{1 + \frac{1}{2}\bar{w}}{x}$$

Performing these calculations for $\bar{w} = 0.155$ gives the values of σc_l and bc_l in the following table (the blade-width distribution, in feet, for a constant c_l of 0.5 is also given):

x	tan φ	K(x)	σc_l	bc_l	b (ft)	$bc_l \Big/ (bc_l)_{0.7R}$
0.1	7.74	0.033	0.0842	0.079	0.158	0.167
.2	3.870	.078	.0967	.182	.364	.386
.3	2.580	.133	.1054	.298	.596	.631
.4	1.935	.185	.1044	.393	.786	.833
.5	1.548	.225	.0952	.449	.898	.952
.6	1.290	.260	.0855	.483	.966	1.023
.7	1.106	.271	.0716	.472	.944	1.000
.8	.968	.257	.0554	.417	.834	.880
.9	.860	.204	.0364	.309	.618	.655
.95	.815	.146	.0241	.216	.432	.458

Dual rotation.- The procedure is repeated for a 12-foot-diameter four-blade dual-rotating propeller for the same design conditions as used for the single-rotating propeller. The following table is obtained for the four-blade dual-rotating propeller (values of κ and ϵ/κ were found from figure 18):

$\bar{w}$	κ	ϵ/κ	P_c
0	0.472	0.589	0
.1	.432	.547	.1002
.2	.398	.519	.211

In this case a plot of P_c against $\bar{w}$ gives a value of $\bar{w} = 0.075$ at $P_c = 0.075$. Therefore,

$$\frac{V}{nD}(1 + \bar{w}) = 2.426$$

$$\kappa = 0.442$$

$$\frac{P_c}{\kappa} = 0.170$$

and

$$\eta_i = 0.964$$

It is seen that the important parameter, the mass-flow coefficient, is 0.442 for the dual-rotating propeller and is only 0.201 for the single-rotating propeller. The efficiency (without drag) is 96.4 percent for the dual-rotating propeller but is only 92.9 percent for the single-rotating propeller.

For the dual-rotating propeller the values of σc_l may be found for the front component from equation (12); thus,

$$\left(\sigma c_l\right)_F = \frac{V}{nD}\frac{1}{\pi x}\frac{(1 + \bar{w})\bar{w} \sin \varphi_o}{1 + \frac{1}{4}\kappa\bar{w} \sin^2\varphi_o} K(x)$$

and for the rear propeller from equation (13)

$$\left(\sigma c_l\right)_R = \frac{V}{nD}\frac{1}{\pi x}\frac{(1 + \bar{w})\bar{w} \sin \varphi_o}{1 + \frac{3}{4}\kappa\bar{w} \sin^2\varphi_o} K(x)$$

Equation (9) gives φ_F by

$$\tan \varphi_F = \frac{V}{nD}\frac{1}{\pi x}\left[1 + \frac{1}{2}\bar{w}\left(1 + \frac{1}{2}\kappa \tan^2\varphi\right)\right]$$

and φ_R is given in equation (11) by

$$\tan \varphi_R = \frac{V}{nD} \frac{1}{\pi x} \left[1 + \frac{1}{2} \bar{w} \left(1 - \frac{1}{2} \kappa \tan^2 \varphi \right) \right]$$

Values of the circulation function $K(x)$ are obtained from figure 8 at the appropriate value of $\frac{V + w}{nD} = \frac{V}{nD}(1 + \bar{w})$. Performing these calculations for $V = 623$, $n = 23$, $D = 12$, $\bar{w} = 0.075$, and $\kappa = 0.442$ gives the values of $\tan \varphi$ and σc_l in the following table:

x	K(x)	$\tan \varphi_F$	$\tan \varphi_R$	$(\sigma c_l)_F$	$(\sigma c_l)_R$	$(bc_l)_F$	$(bc_l)_R$
0.1	0.575	10.768	4.145	0.326	0.321	0.616	0.606
.3	.565	2.608	2.363	.0995	.0985	.564	.557
.4	.551	1.916	1.812	.0692	.0683	.522	.515
.5	.539	1.518	1.465	.0501	.0496	.472	.467
.6	.530	1.258	1.227	.0370	.0366	.418	.414
.7	.455	1.075	1.056	.0268	.0267	.354	.352
.8	.398	.939	.926	.0191	.0190	.288	.287
.9	.307	.833	.824	.0122	.0122	.207	.207
.95	.233	.789	.781	.0085	.0085	.152	.152

A comparison of the optimum distribution of bc_l along the blade for the dual-rotating propeller from this table with the optimum distribution for the single-rotating propeller as given in the preceding section shows that, if approximately constant c_l is absorbed along the blade, wide differences in blade plan form will result for the two propellers designed for the same operating condition. For the operating conditions selected, the maximum bc_l for the single-rotating propeller occurs near the 0.6 radius and tapers rapidly towards the tip and the hub, being only slightly over 16 percent of its maximum value at the 0.1 radius. On the other hand, the minimum value of bc_l for optimum distribution for the dual-rotating propeller occurs at the propeller tip and progressively increases toward the inner radii. The value of bc_l at the 0.1 radius is four times its value at the 0.95 radius.

Since the design of the dual-rotating propeller calls for high loading over the inner sections, the efficiency of the dual-rotating propeller is less susceptible to compressibility losses which normally occur near the propeller tip for operation at high tip Mach numbers. The compressibility losses may be reduced by reducing the width of these sections or by reducing the operating lift coefficient.

Effect of blade drag on efficiency.- The loss in efficiency due to the profile drag of the blades can be calculated from equations (20) to (22) if the blade-width distribution and profile-drag coefficients at the operating c_l are known. Inasmuch as structural requirements may determine the shape of the blade, especially over the inner radii, only one example is given. The equations, however, may be applied to any plan form. The example selected is for the four-blade single-rotating propeller on which the induced efficiency has been previously calculated. The shank sections of the propeller blade were assumed to be round, similar to the Hamilton Standard Propeller No. 3155-6 and the blade plan form from $x = 0.3$ to $x = 1.0$ was made optimum for a c_l of 0.5. The profile-drag coefficients for the several radii are the same as given in reference 7 for the Hamilton Standard Propeller No. 3155-6 which has Clark Y sections and are given in the following table. It is assumed that a spinner covers the inner 0.2 of the radius. The distribution of σc_l with x and of $\sin \varphi$ with x have been included in the table:

x	σc_l	σ	c_d	$\sin \varphi$	$\frac{\sigma c_d}{\sin \varphi} x$	$\frac{\sigma c_d}{\sin \varphi} x^3$
0.2	0.0967	0.1934	0.400	0.968	0.01600	0.00064
.3	.1054	.2108	.100	.932	.00697	.00061
.4	.1044	.2088	.020	.889	.00188	.00030
.5	.0952	.1904	.010	.840	.00113	.00028
.6	.0855	.1710	.008	.790	.00104	.00037
.7	.0716	.1432	.007	.742	.00095	.00046
.8	.0554	.1108	.006	.696	.00077	.00049
.9	.0364	.0728	.006	.652	.00060	.00049

Performing the integrations and substituting in the formulas gives for rotational-drag-loss coefficient

$$t_r = \frac{2}{\lambda_g^2} \int_{0.2}^{1.0} \frac{\sigma c_d}{\sin \varphi} x^3 \, dx$$

$$= \frac{2}{0.516}(0.000348) = 0.0014$$

and for the axial-drag-loss coefficient

$$t_a = 2\int_{0.2}^{1.0} \frac{\sigma c_d}{\sin \varphi} x \, dx$$

$$= 2(0.00213) = 0.0043$$

The induced thrust coefficient has been given by equation (14) as

$$c_s = 2\kappa\bar{w}\left[1 + \bar{w}\left(\frac{1}{2} + \frac{\epsilon}{\kappa}\right)\right]$$

$$= 2(0.201)(0.155)\left[1 + 0.155\left(\frac{1}{2} \tau\ 0.29\right)\right] = 0.0700$$

and the induced power coefficient by equation (16) as

$$P_c = 2\kappa\bar{w}(1 + \bar{w})\left(1 + \frac{\epsilon}{\kappa}\bar{w}\right)$$

$$= 2(0.201)(0.155)(1.155)(1.045) = 0.0754$$

The induced efficiency is

$$\eta_i = \frac{c_s}{P_c}$$

$$= \frac{0.0700}{0.0754} = 0.929$$

With drag included, the total thrust is given by

$$c_{s_T} = c_s - t_a$$

$$= 0.0700 - 0.0043 = 0.0657$$

and

$$P_{c_T} = P_c + t_r$$

$$= 0.0754 + 0.0014 = 0.0768$$

The efficiency is

$$\eta = \frac{c_{s_T}}{P_{c_T}} = \frac{0.0657}{0.0768} = 0.855$$

Thus it is seen that the blade drag of the magnitude given in the preceding table reduces the propeller efficiency from 92.9 percent to 85.5 percent for the propeller operating conditions given.

CONCLUDING REMARKS

A comparison of Theodorsen's propeller theory with the conventional vortex theory shows that the optimum load distribution along the blade for single-rotating propellers obtained by the two theories is essentially identical and as a result the optimum efficiencies are the same for a given operating condition. Theodorsen's theory has the advantage, however, that the optimum efficiency for any design condition can be obtained quickly and accurately by the use of the mass coefficient κ without any laborious calculations and before the final design is made.

The distribution of the circulation function $K(x)$ for the idealized dual-rotating propeller is radically different from the existing values for the single-rotating propeller that have been previously used for the dual-rotating propeller. Also, the mass coefficient κ for the dual-rotating propeller is larger than the sum of the values for two single-rotating propellers. These quantities, which are not available from mathematical computations but are obtained from the electrical-analogy method of Theodorsen, are used herein for obtaining the optimum load distribution along the blade for the dual-rotating propeller.

Langley Aeronautical Laboratory
National Advisory Committee for Aeronautics
Langley Field, Va.

REFERENCES

1. Theodorsen, Theodore: The Theory of Propellers. I - Determination of the Circulation Function and the Mass Coefficient for Dual-Rotating Propellers. NACA Rep. No. 775, 1944.

2. Theodorsen, Theodore: The Theory of Propellers. II - Method for Calculating the Axial Interference Velocity. NACA Rep. No. 776, 1944.

3. Theodorsen, Theodore: The Theory of Propellers. III - The Slipstream Contraction with Numerical Values for Two-Blade and Four-Blade Propellers. NACA Rep. No. 777, 1944.

4. Theodorsen, Theodore: The Theory of Propellers. IV - Thrust, Energy, and Efficiency Formulas for Single- and Dual-Rotating Propellers with Ideal Circulation Distribution. NACA Rep. No. 778, 1944.

5. Goldstein, Sydney: On the Vortex Theory of Screw Propellers. Proc. Roy. Soc. (London), ser. A, vol. 123, no. 792, April 6, 1929, pp. 440-465.

6. Lock, C. N. H., and Yeatman, D.: Tables for Use in an Improved Method of Airscrew Strip Theory Calculation. R. & M. No. 1674, British A.R.C., 1935.

7. Crigler, John L., and Talkin, Herbert W.: Charts for Determining Propeller Efficiency. NACA ACR No. L4I29, 1944.

8. Glauert, H.: Airplane Propellers. The Vortex Theory. Vol. IV of Aerodynamic Theory, div. L, ch. VI, sec. 1, W. F. Durand, ed., Julius Springer (Berlin), 1935, p. 231.

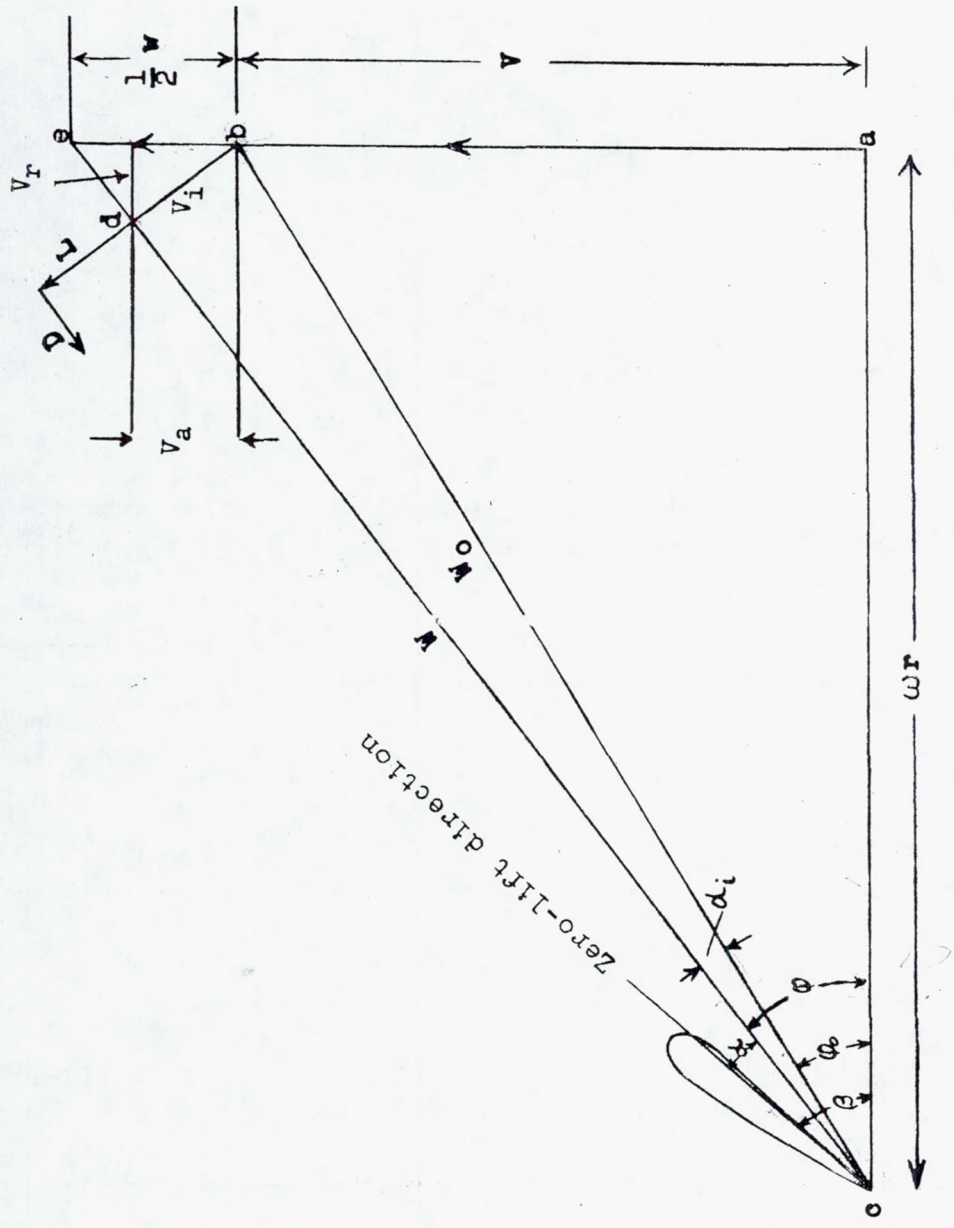


Figure 1.- Velocity diagram for single-rotating propeller.

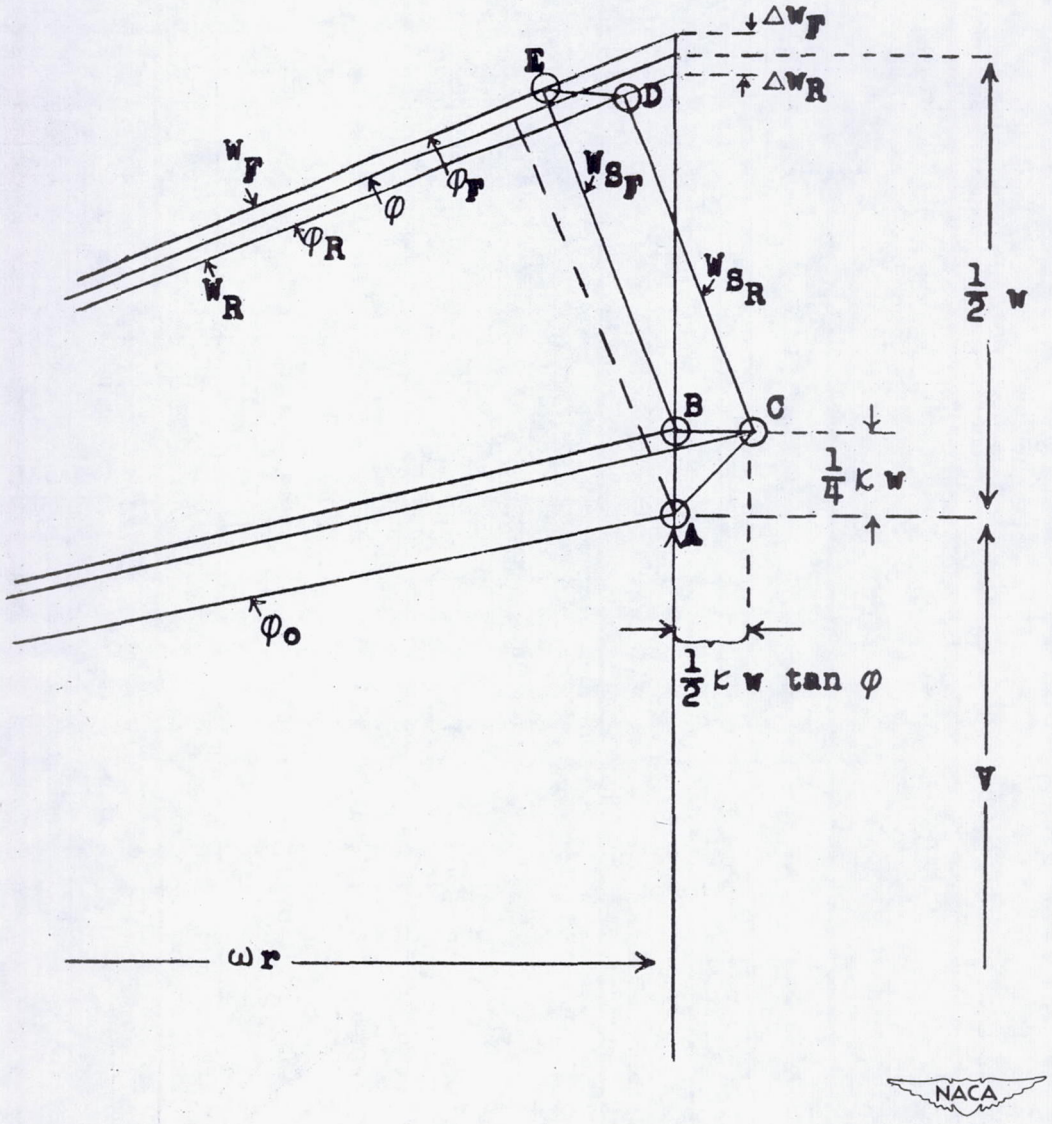


Figure 2.- Velocity diagram for dual-rotating propeller.

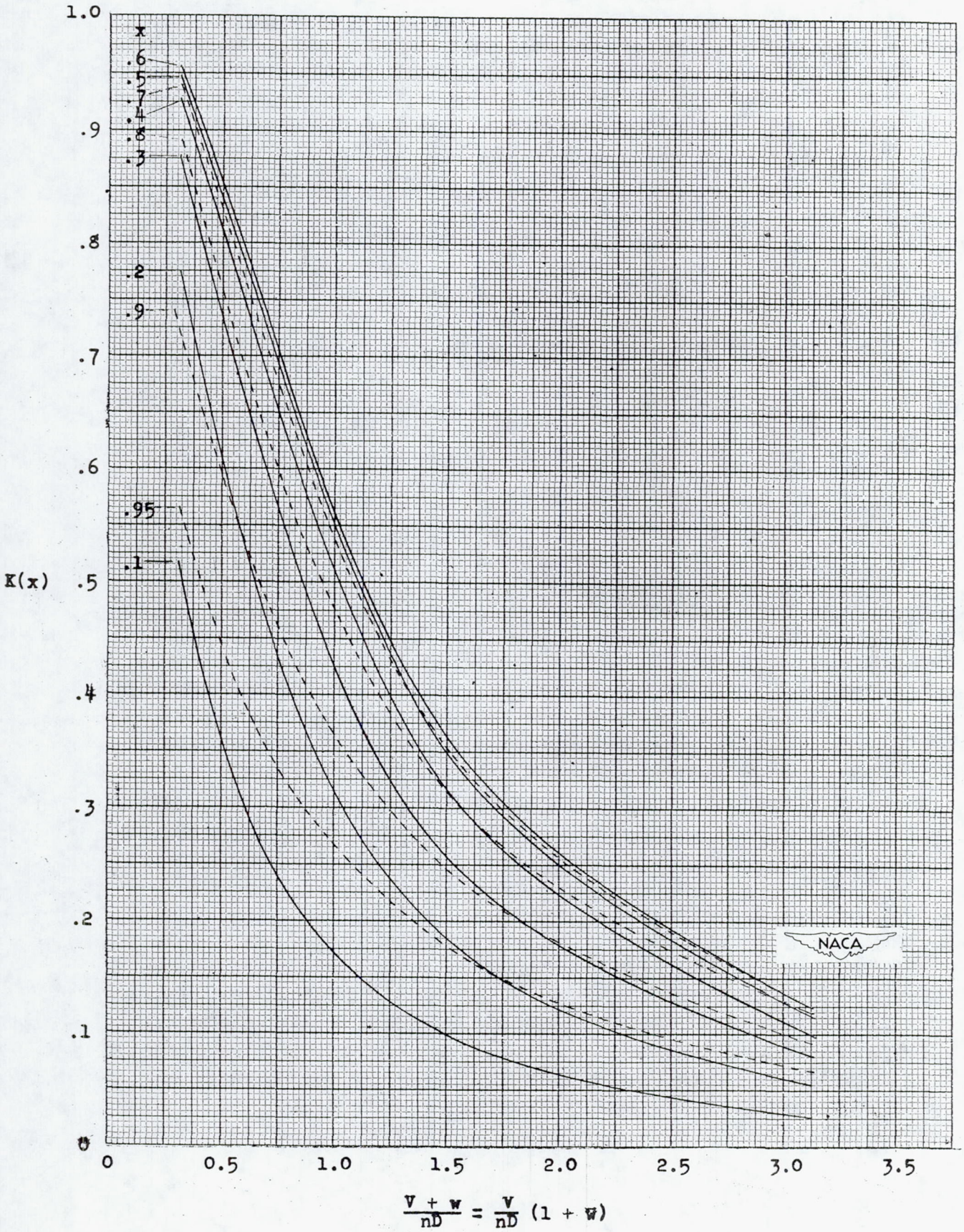


Figure 3.- Circulation function K(x) for two-blade single-rotating

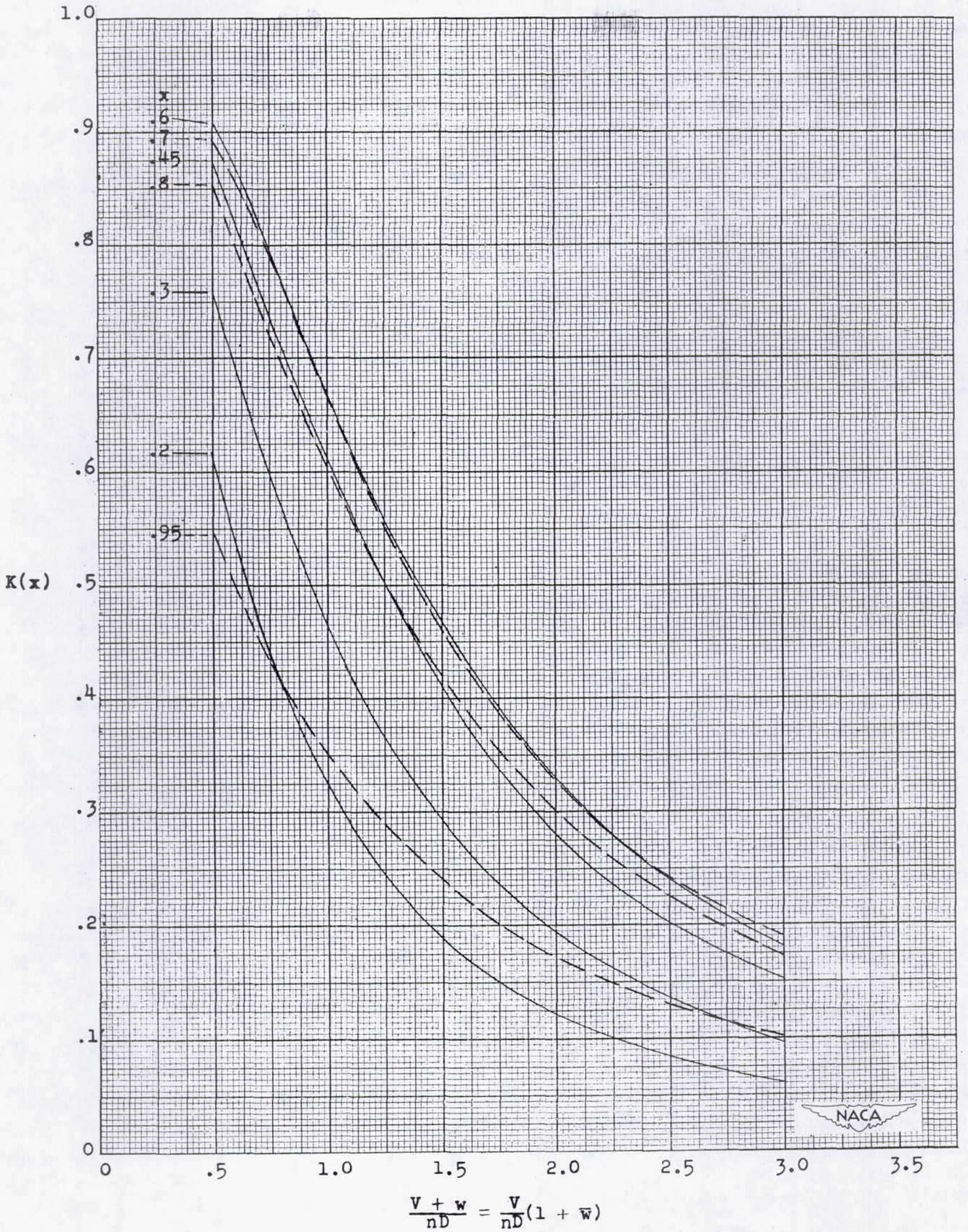


Figure 4.- Circulation function K(x) for three-blade single-rotating propeller (reference 6).

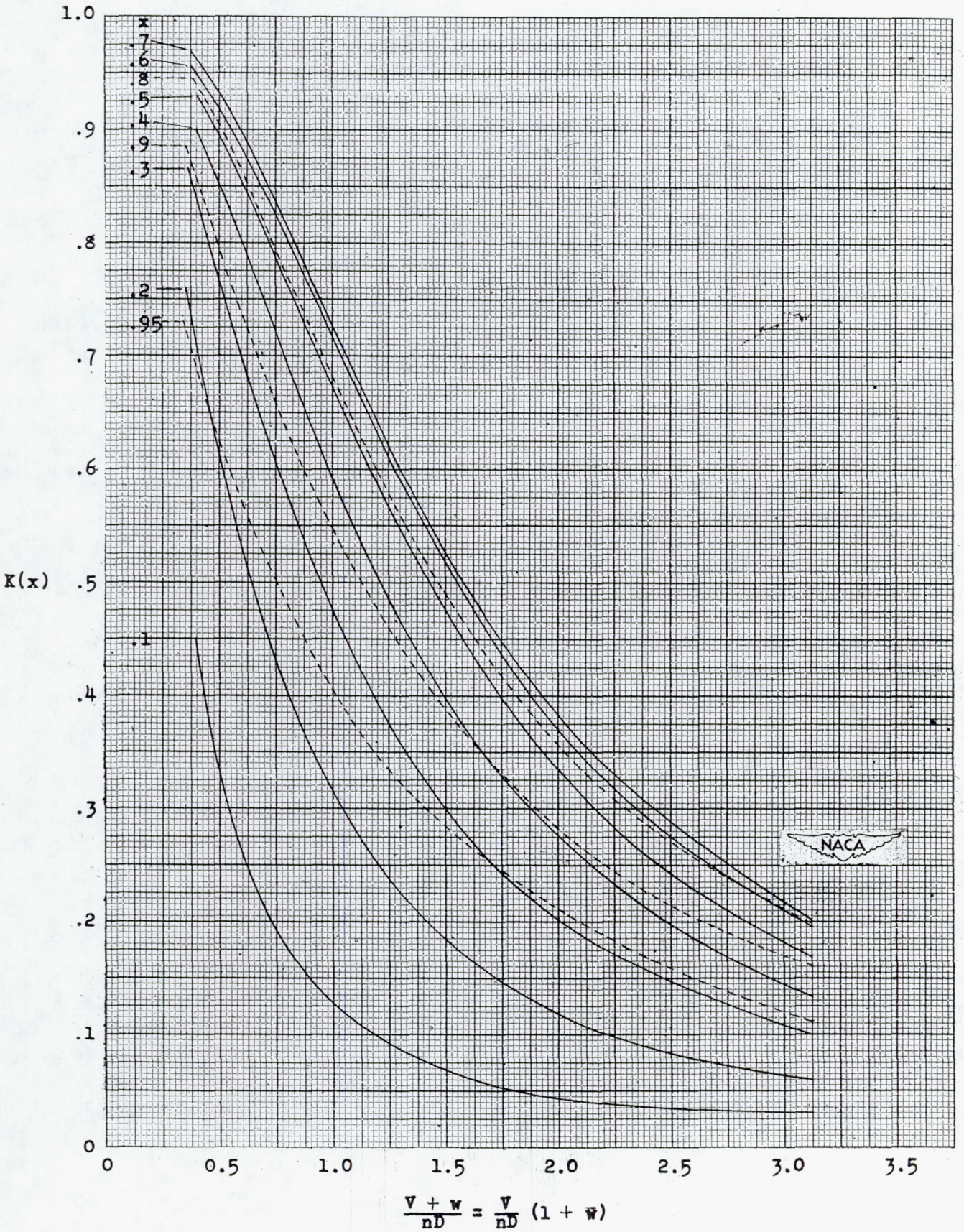


Figure 5.- Circulation function K(x) for four-blade single-

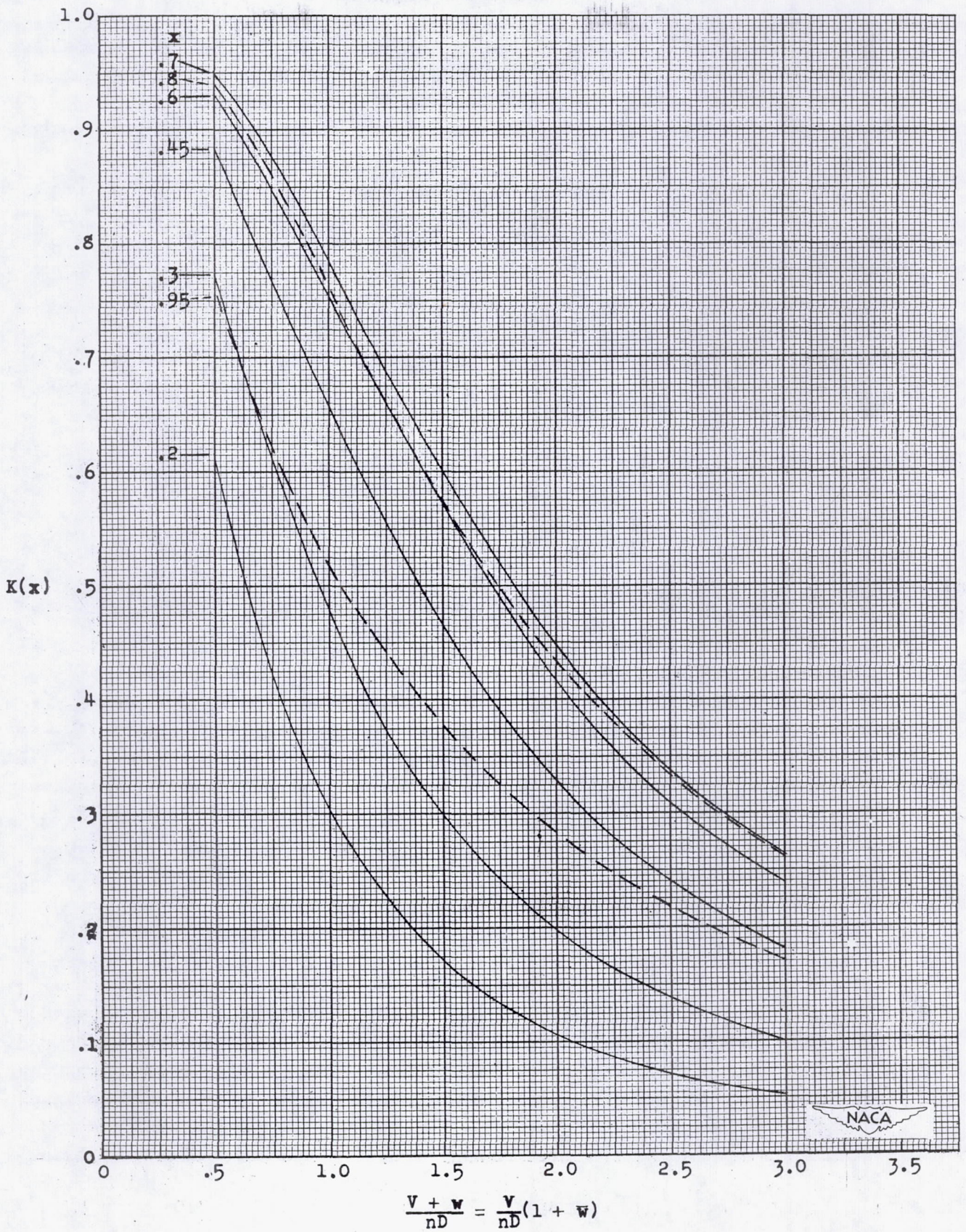


Figure 6.- Circulation function K(x) six-blade single-

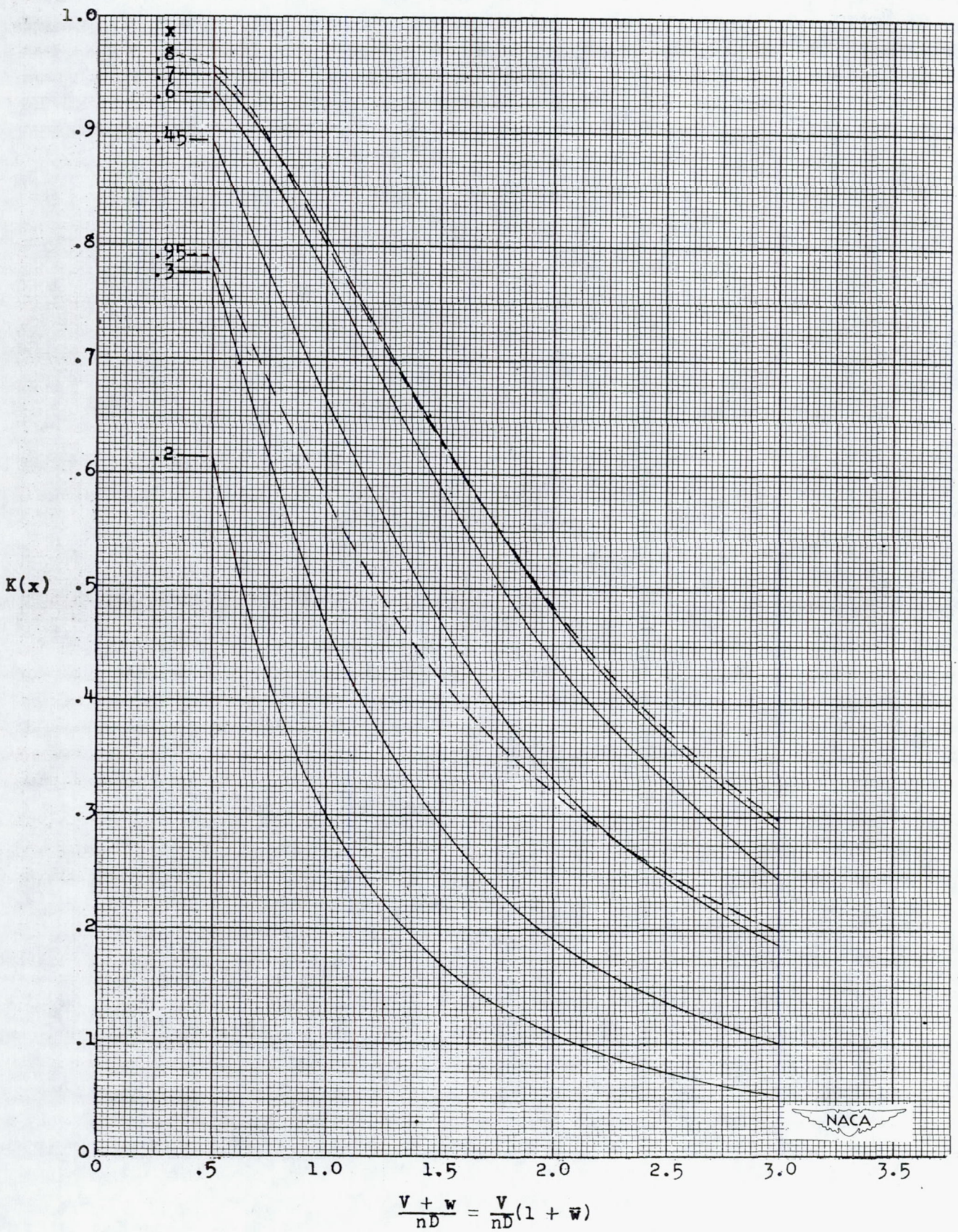


Figure 7.- Circulation function K(x) for eight-blade single-rotating propeller.

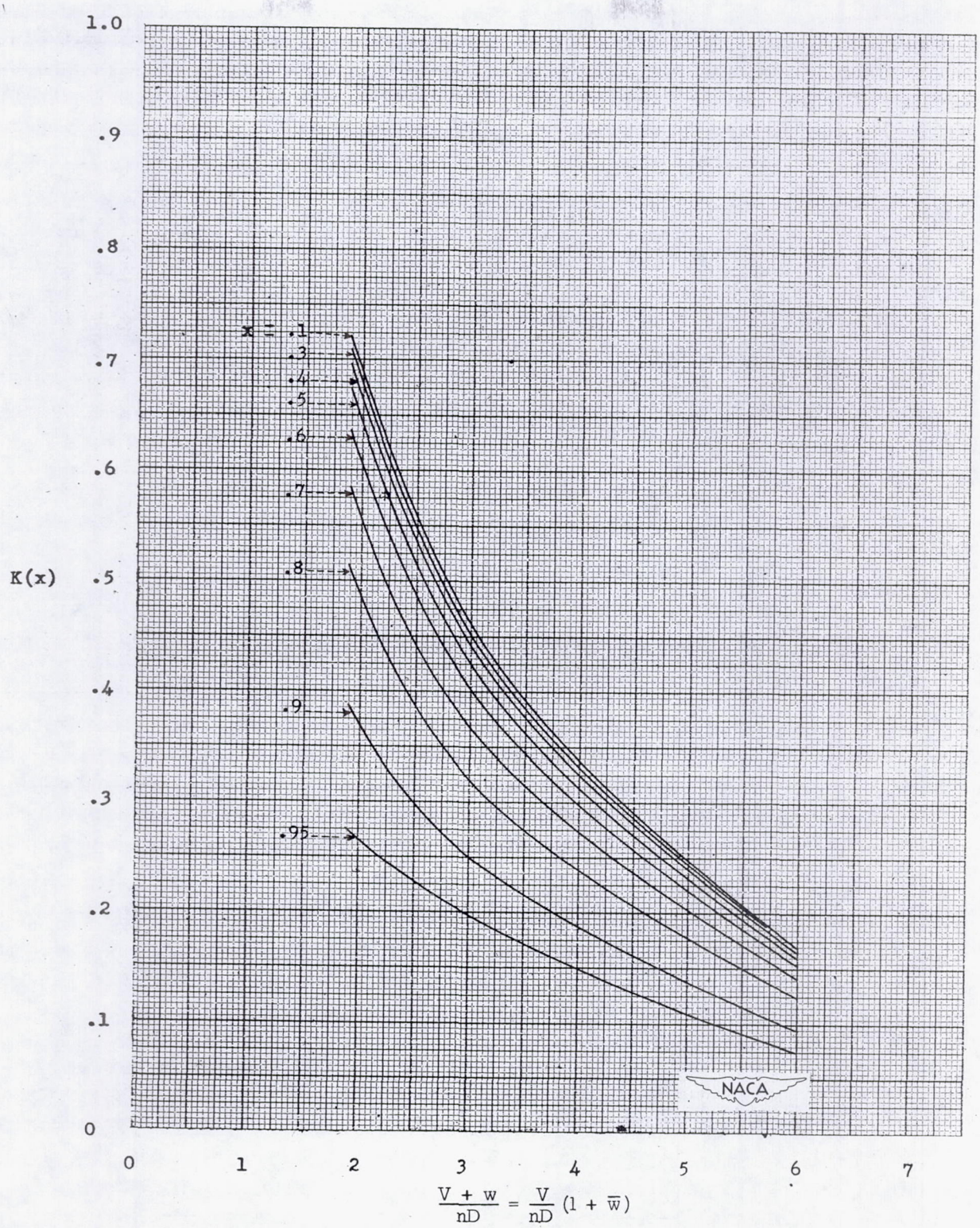


Figure 8.- Circulation function K(x) for four-blade dual-rotating propeller (reference 1).

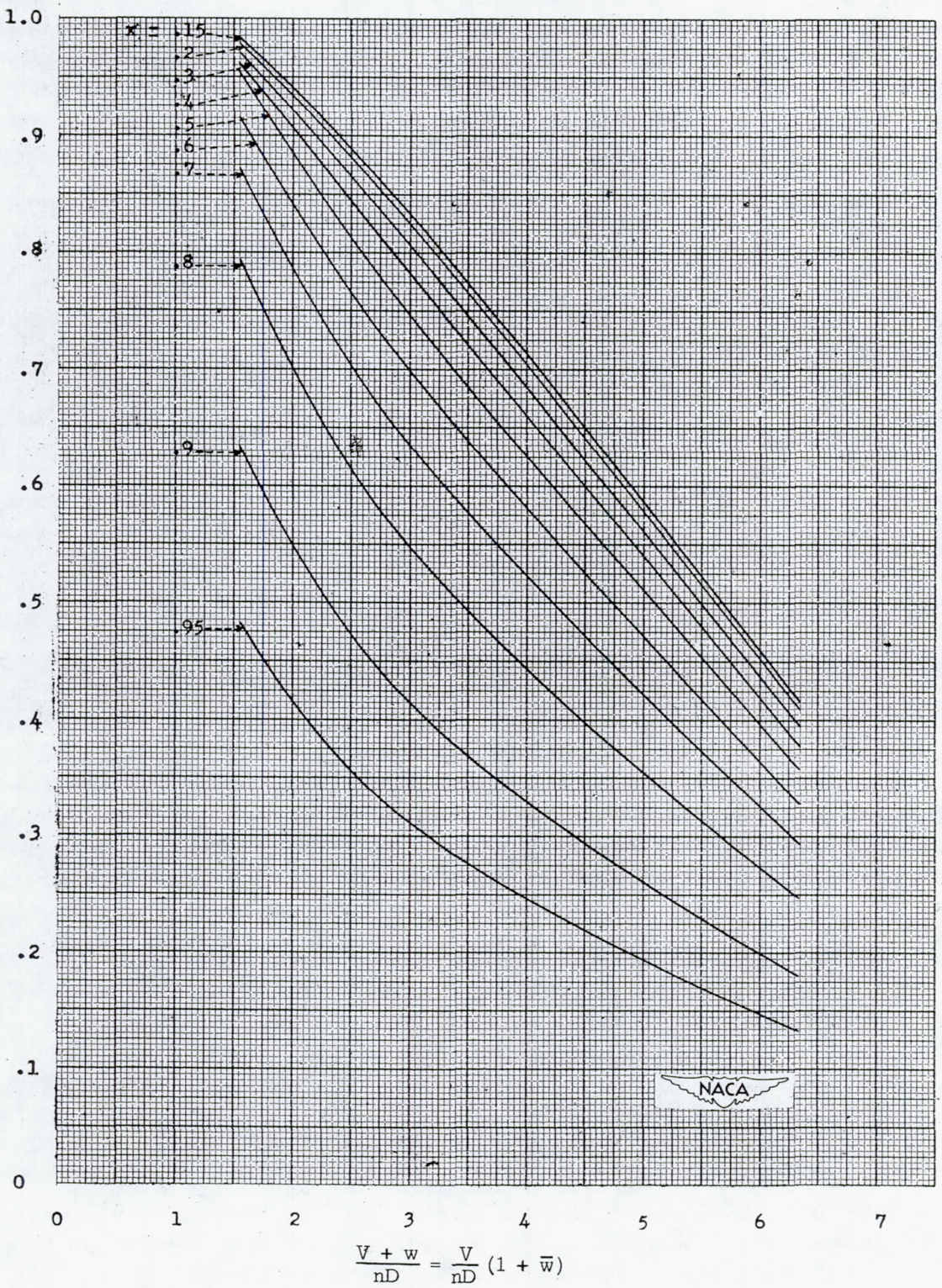


Figure 9.- Circulation function K(x) for eight-blade dual-rotating propeller (reference 1).

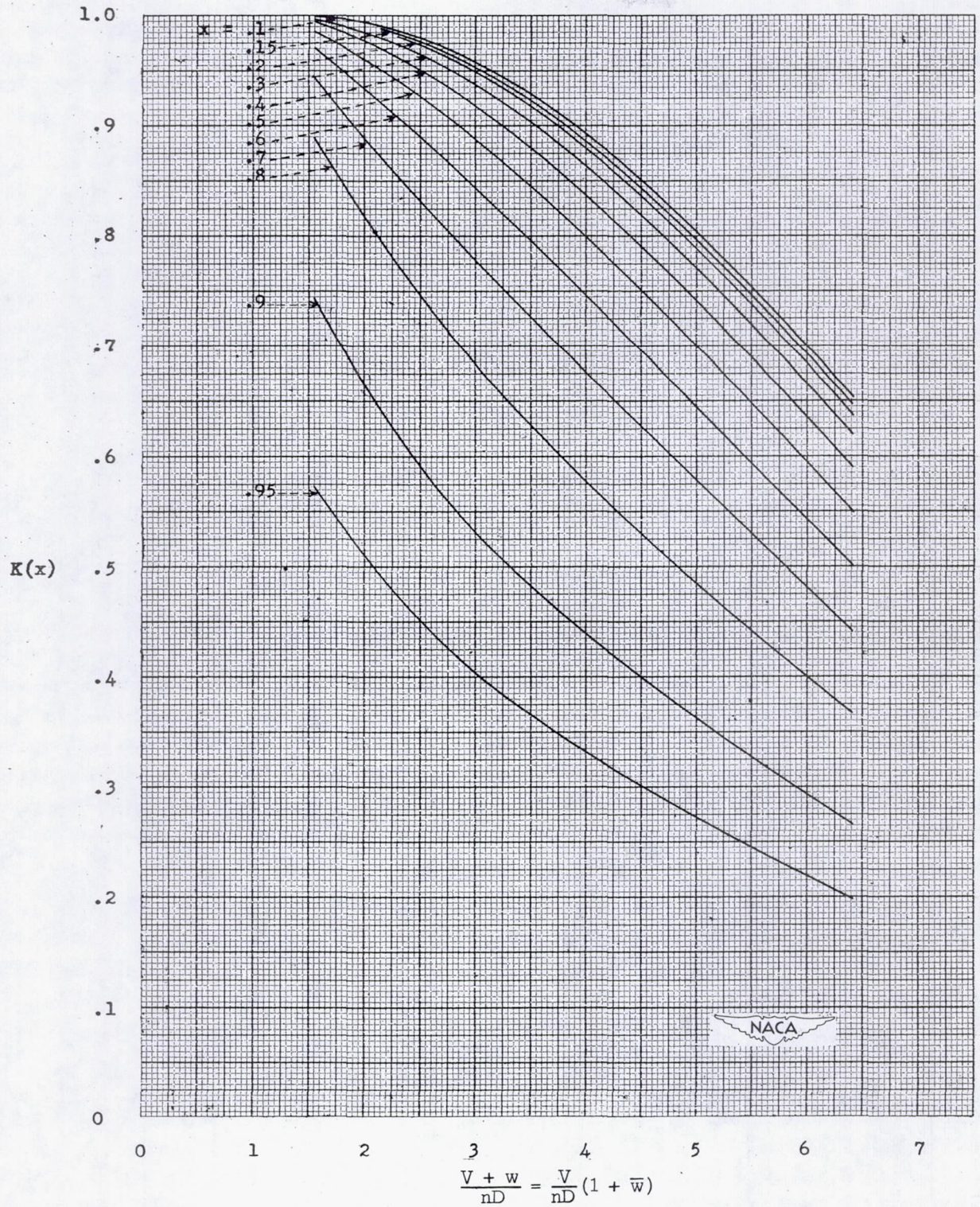


Figure 10.- Circulation function K(x) for twelve-blade dual-rotating propeller (reference 1).

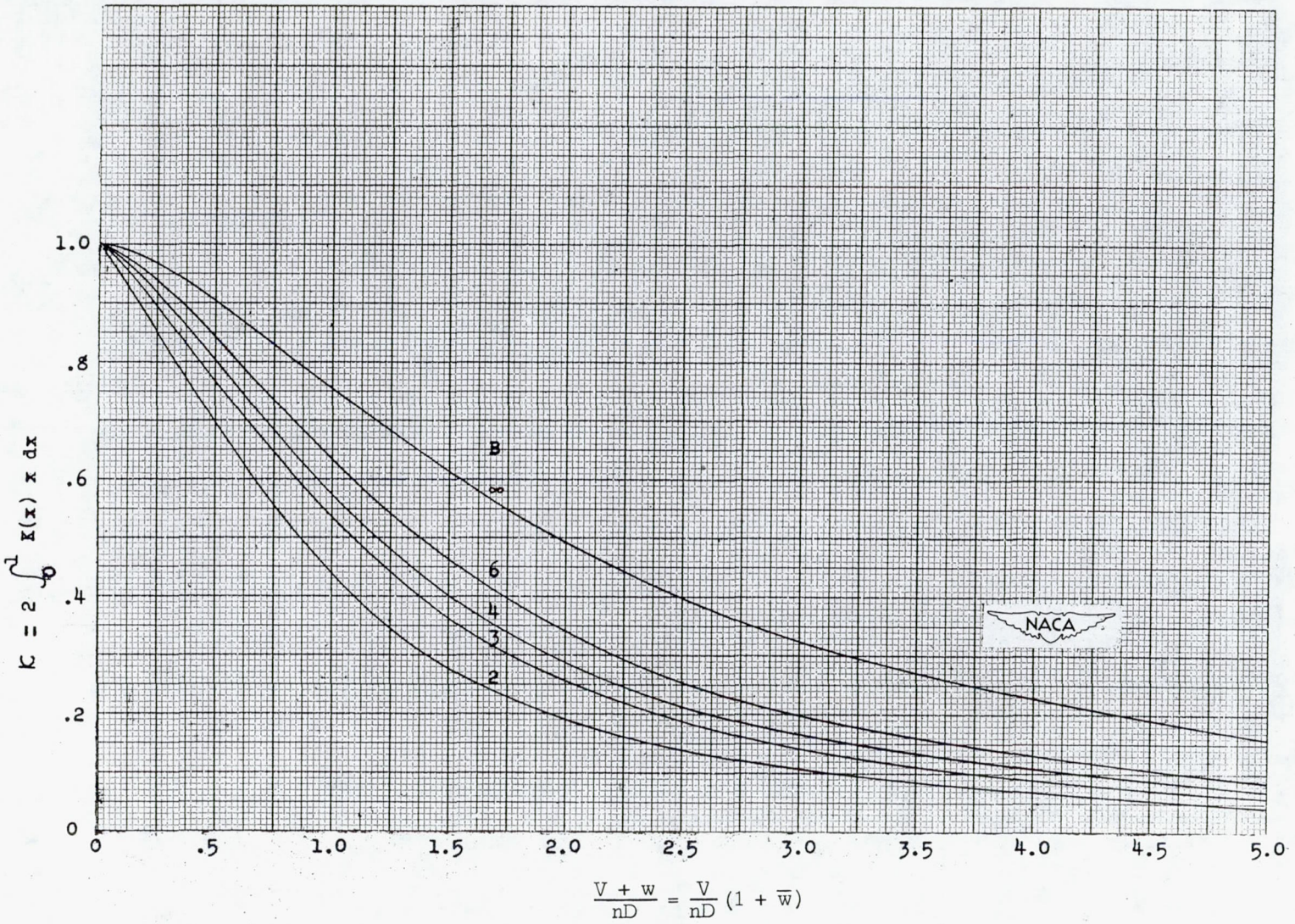


Figure 11- Mass coefficient k against $\frac{V + w}{nD}$ for various numbers of blades for single-rotating propellers.

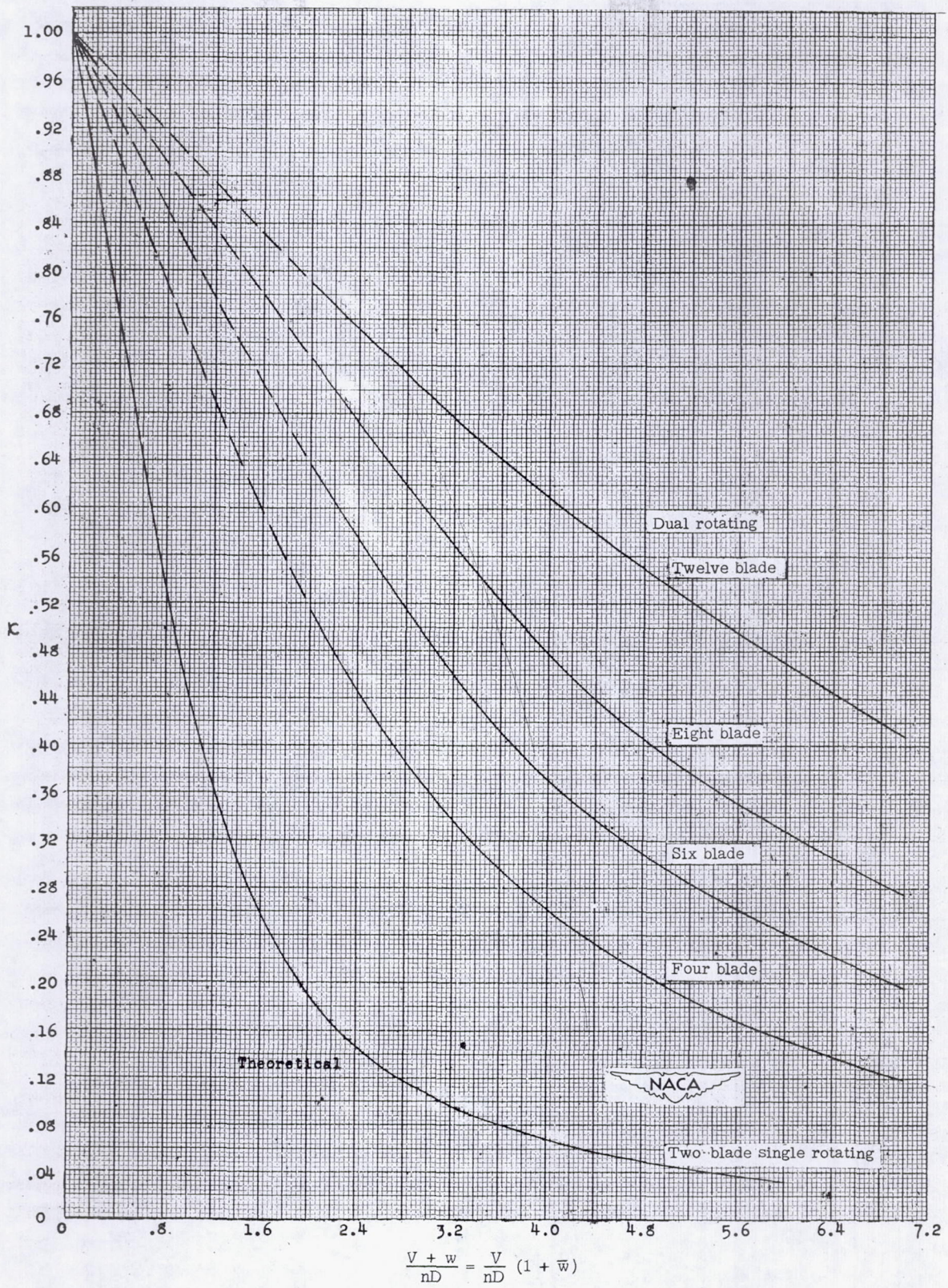


Figure 12.- Measured values of mass coefficient κ for dual-rotating propellers with various numbers of blades. Two-blade single-rotating propeller included for comparison (reference 1).

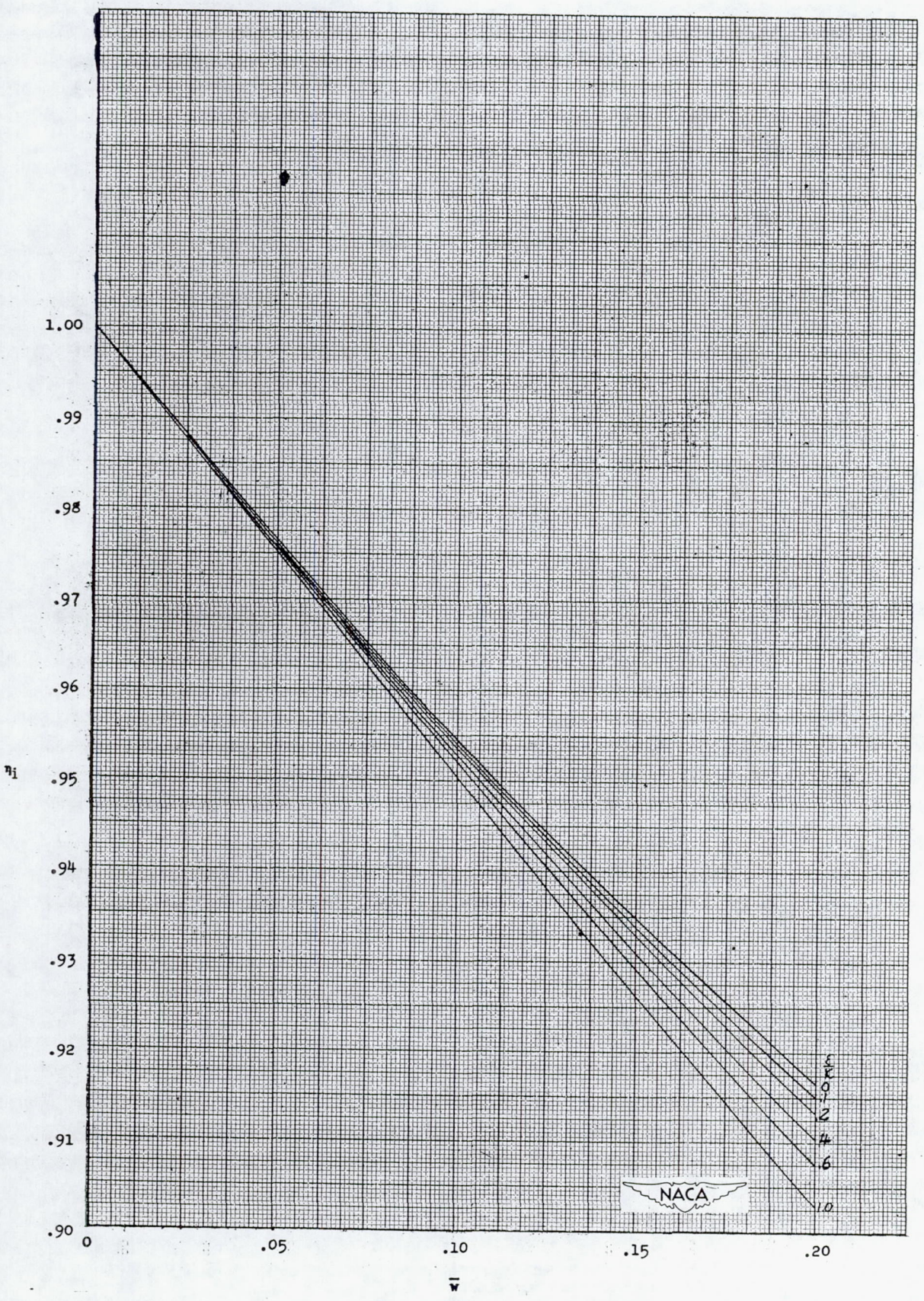


Figure 13.- Propeller efficiency against $\bar{w}$ (reference 4).

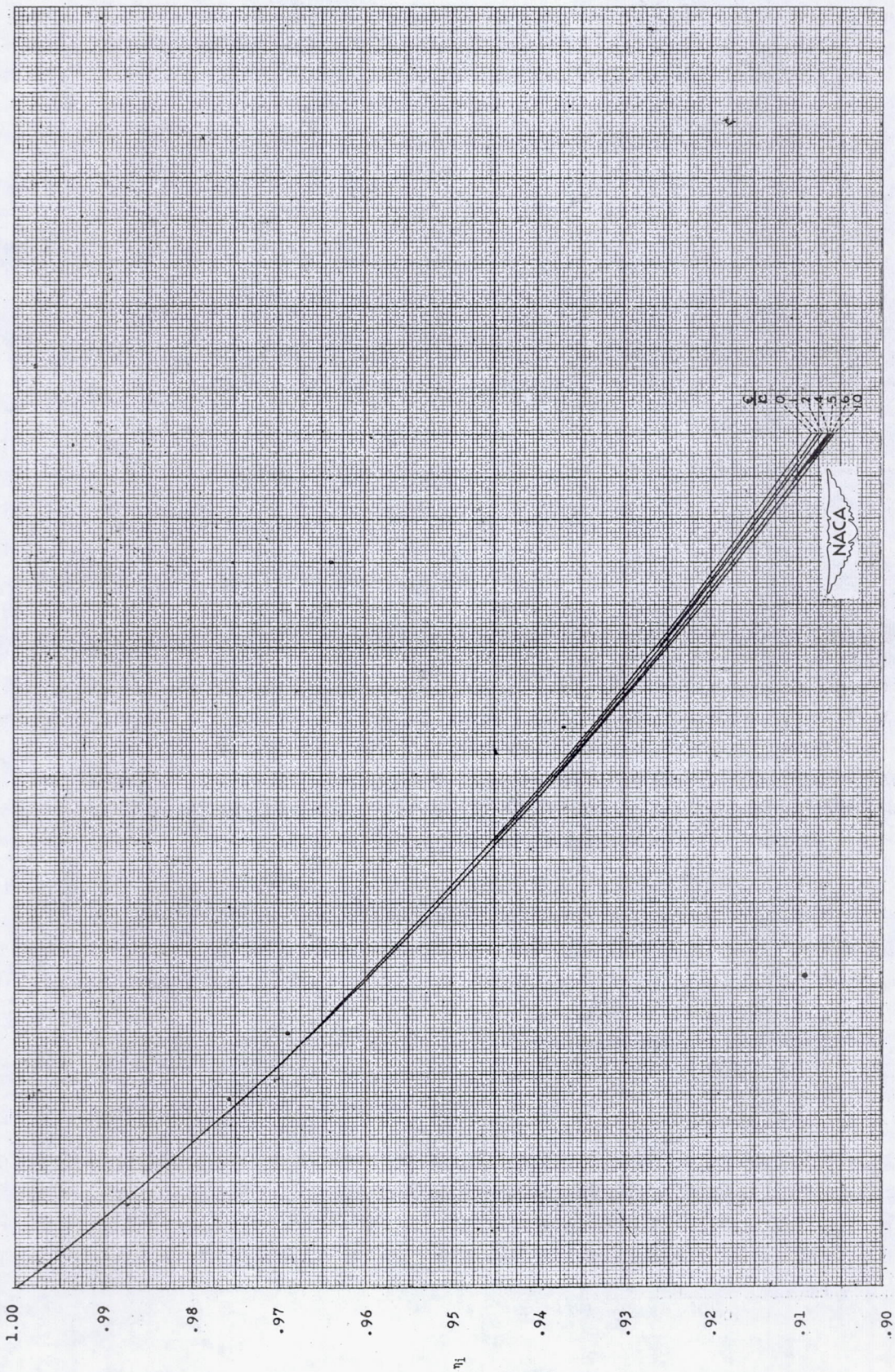


Figure 14.- Propeller efficiency against c_s/κ (reference 4).

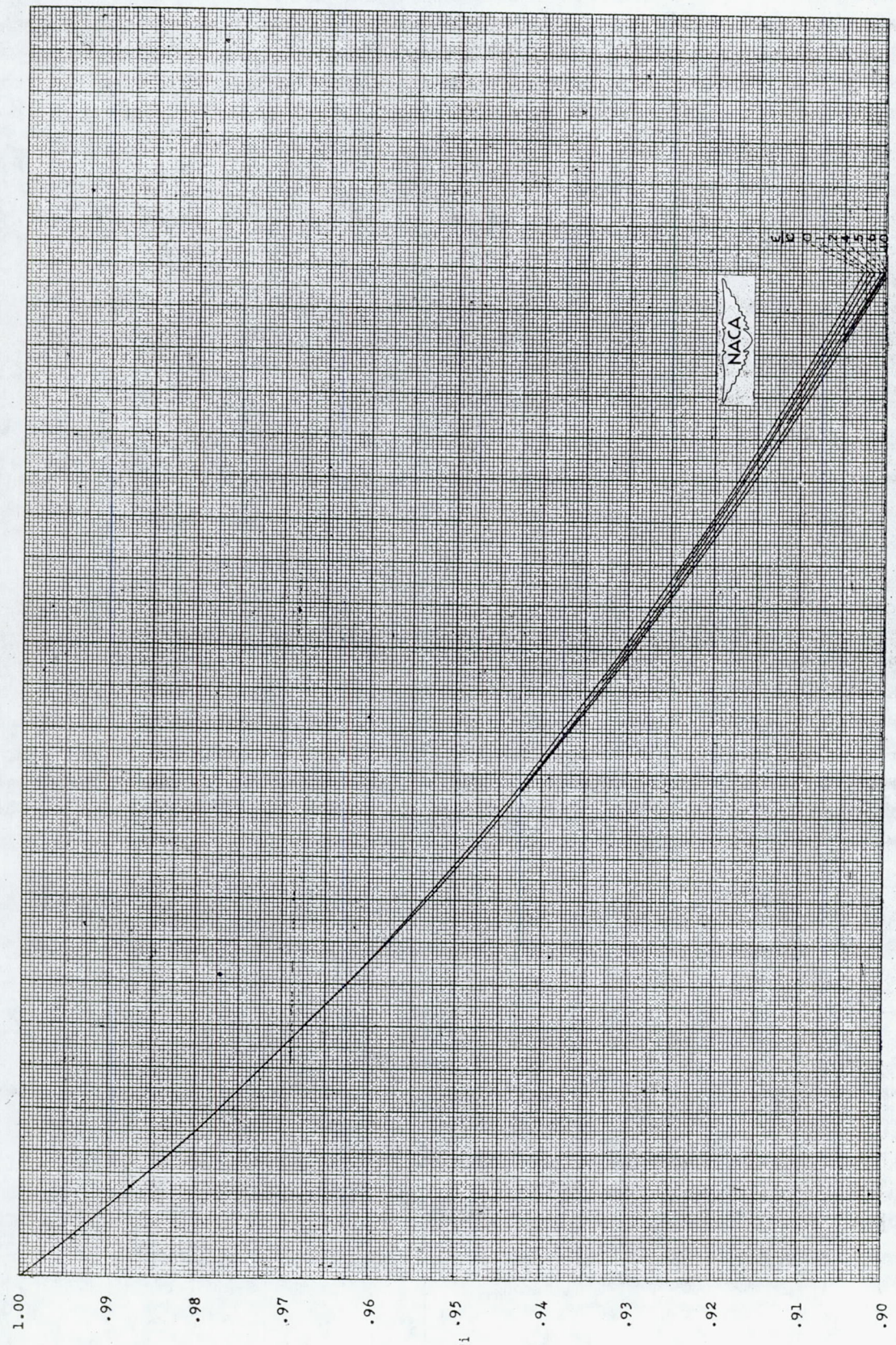


Figure 15.- Propeller efficiency against P_c/κ.

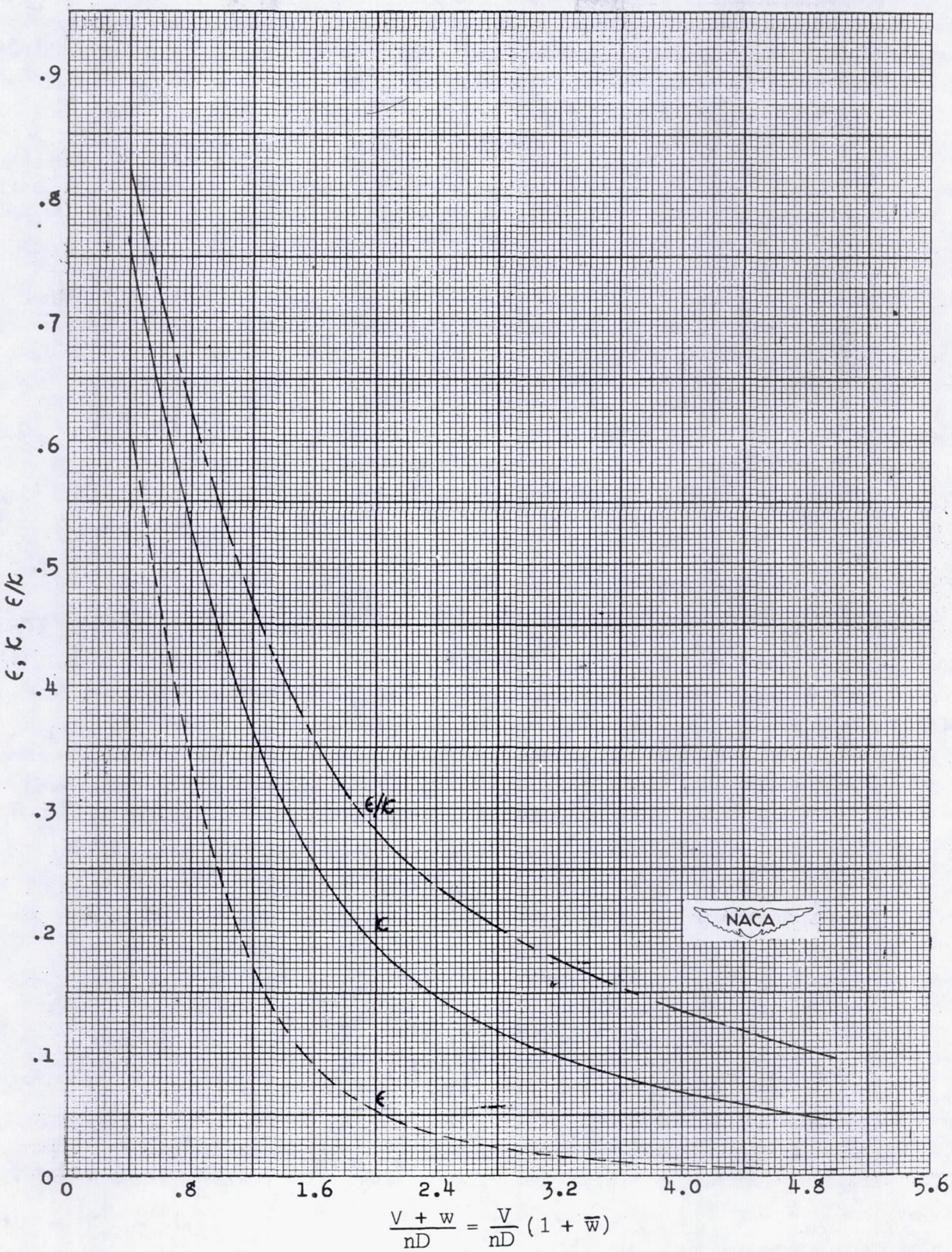


Figure 16.- Values of ϵ and κ for two-blade single-rotating propeller.

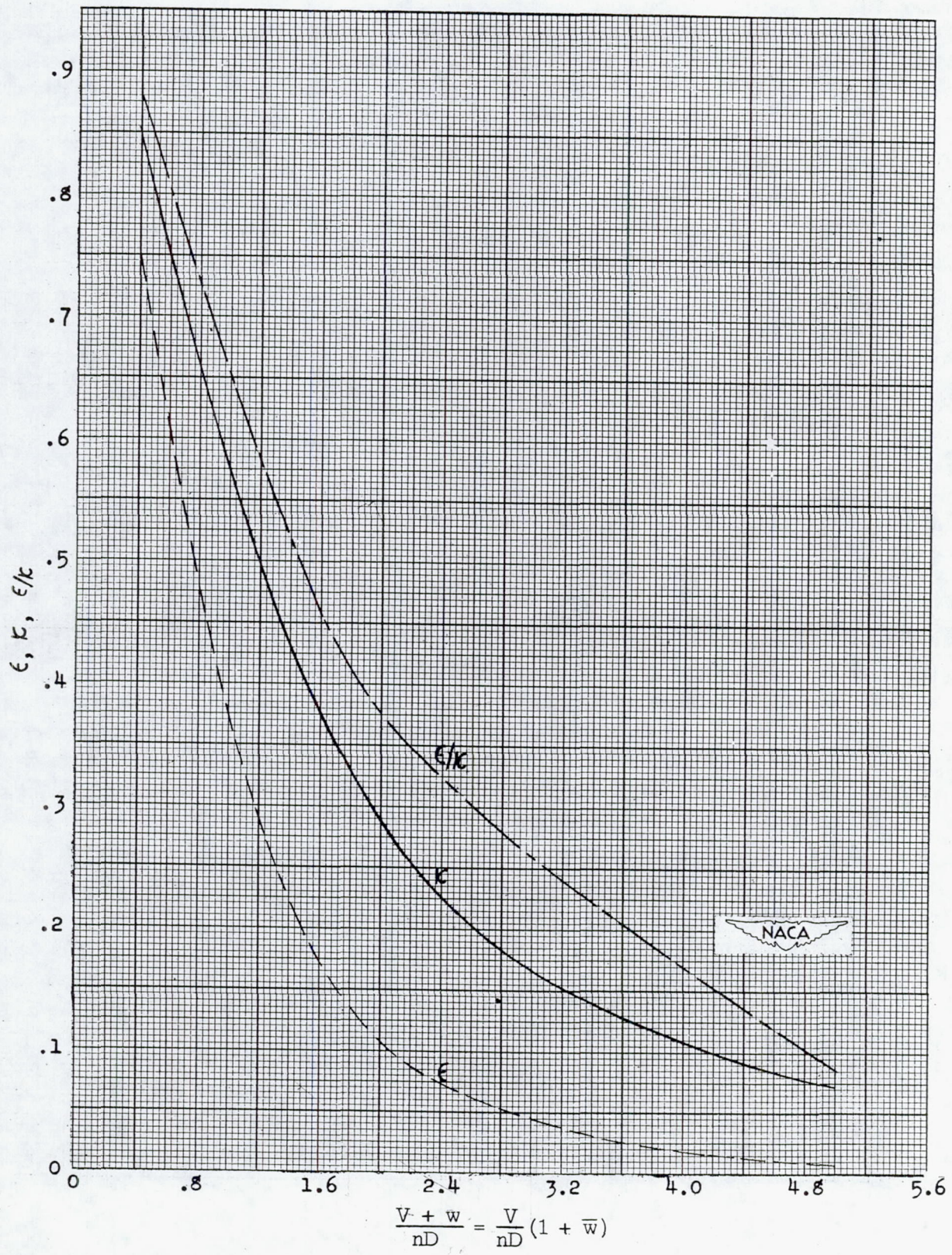


Figure 17.- Values of ϵ and κ for four-blade single-rotating propeller.

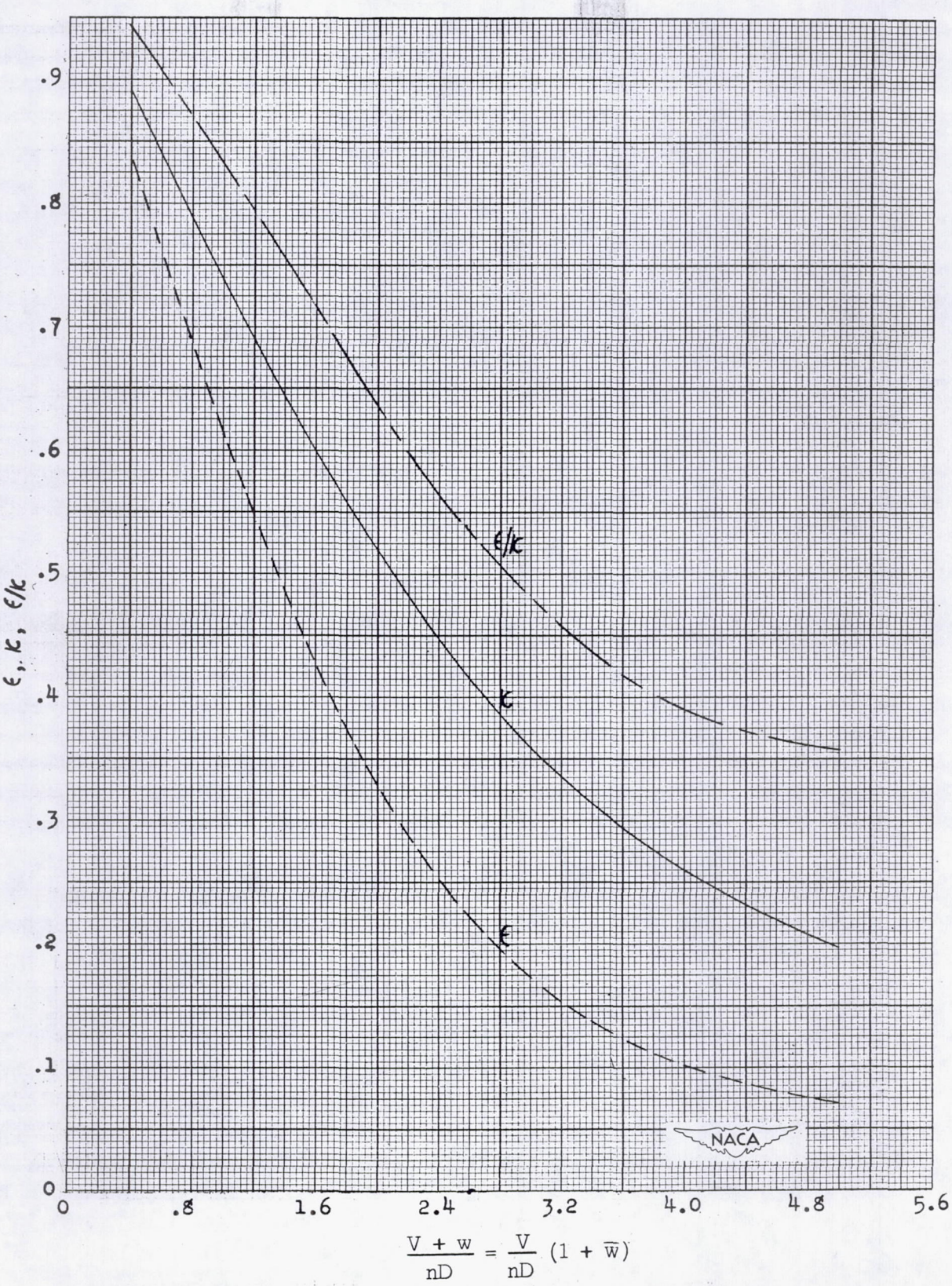


Figure 18.- Values of ϵ and κ for four-blade dual-rotating propeller.

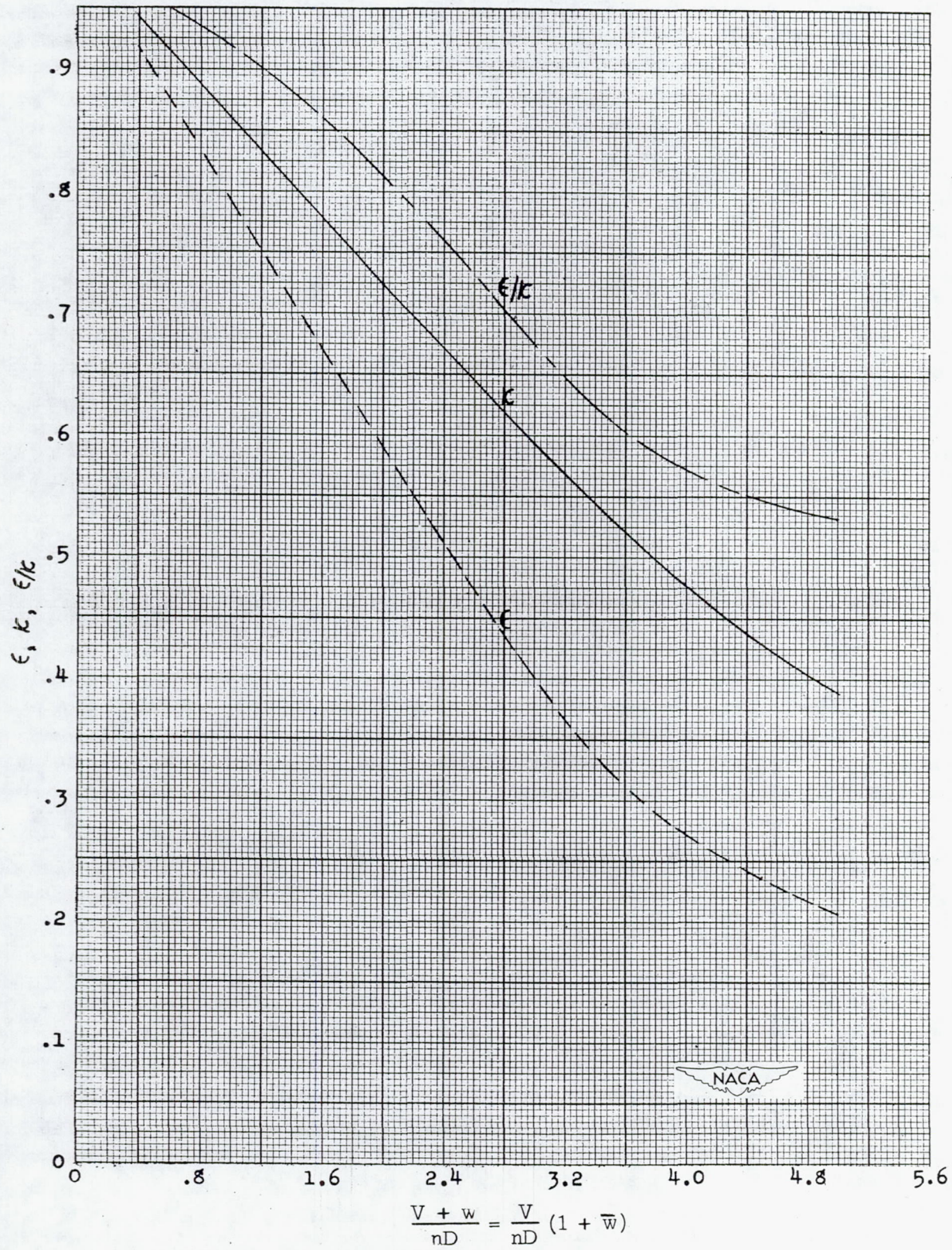


Figure 19.- Values of ϵ and κ for eight-blade dual-rotating propeller.

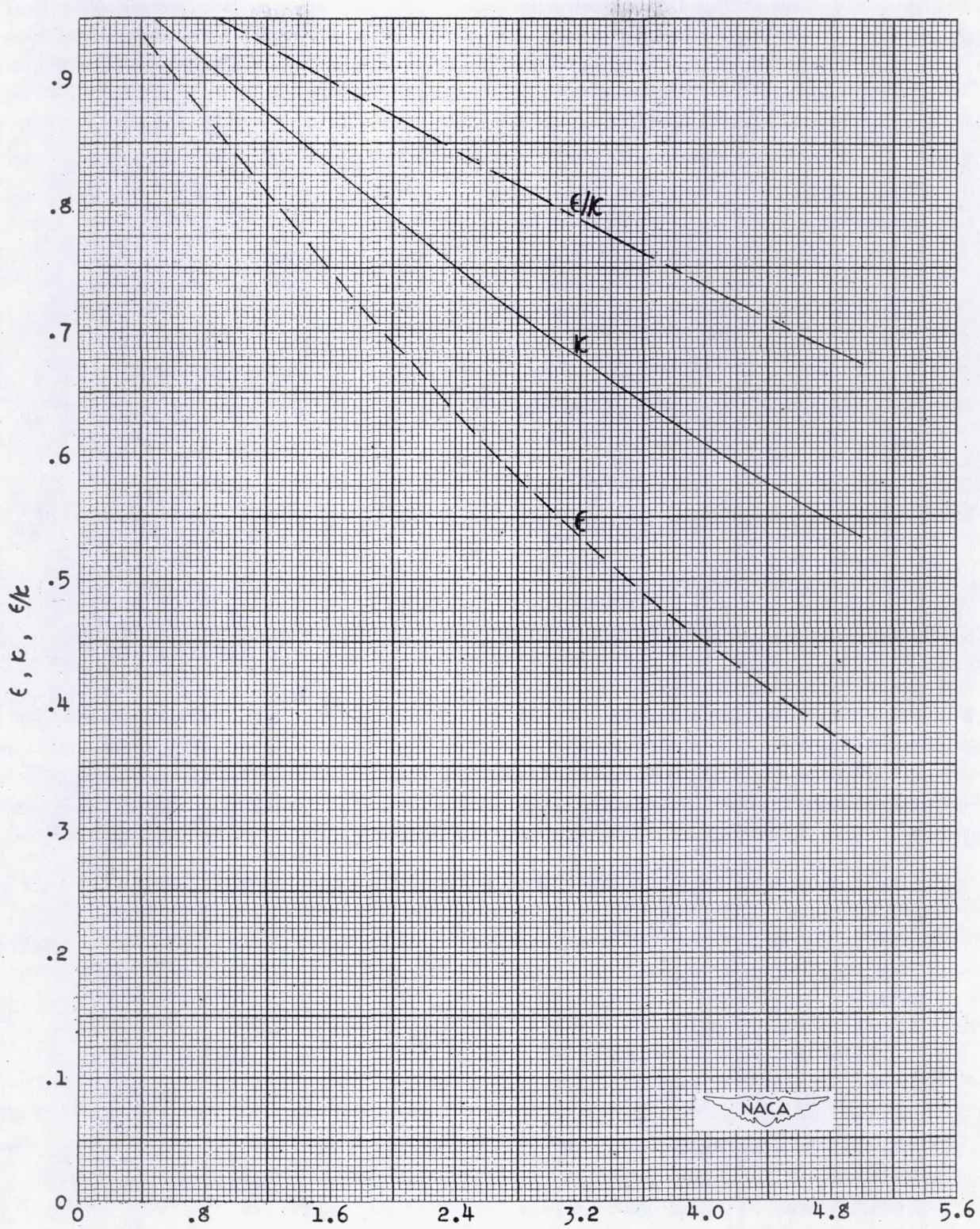


Figure 20.- Values of ϵ and κ for twelve-blade dual-rotating propeller.